Numerical modelling of strain localisation

Panos Papanastasiou[1] and Antonis Zervos[2]

[1]University of Cyprus

[2]University of Southampton

Introduction
Motivation
The problem One way out Outline of the talk

A Gradient Plasticity

Gradient Elastoplasticity

Outlook

Introduction

All materials have microstructure!

- Conventional constitutive models ignore this fact.
- But what if microstructure dominates the behaviour?
  - Deformation localization in thin bands.
  - Scale effects.

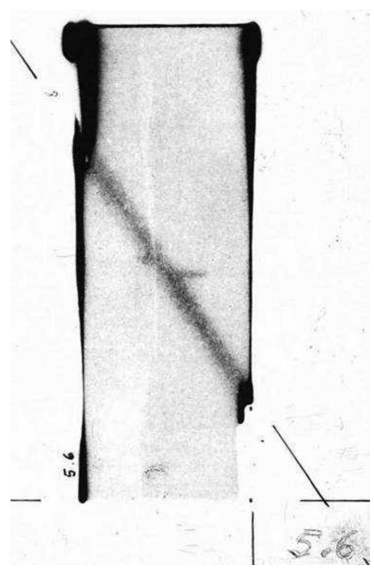

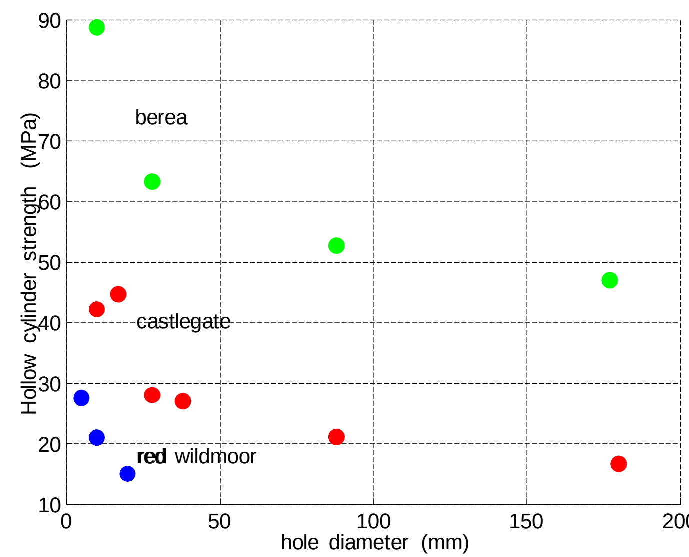

Photos courtesy of Q. Ni & I. Vardoulakis. Data courtesy of E. Papamichos.

Introduction
Motivation
The problem
One way out
Outline of the talk
A Gradient Plasticity
Gradient Elastoplasticity
Outlook

Motivation

Model localisation & scale effect in strain-softening materials

i.e. materials that lose strength as they strain.

- Shearbands in dense sands and overconsolidated clays.
  - Progressive failure of slopes and embankments.
- Localised failure in concrete and rocks.
  - Formation of breakouts in deep boreholes.
- Necking in metals.

...But is that not straight-forward to do with finite elements/differences?

Unfortunately it is far from straight-forward.

Micro-mechanical modelling

- Failure in geomaterials takes place in localized deformation in shear bands
- Modelling localization of deformation requires material softening
- Softening in classical plasticity models results in mesh sensitivity of FE analysis
- Regularized the problem using higher order theories with microstructure, e.g. Cosserat, gradient plasticity, …
- Internal length: determines the shear band thickness and scale effect

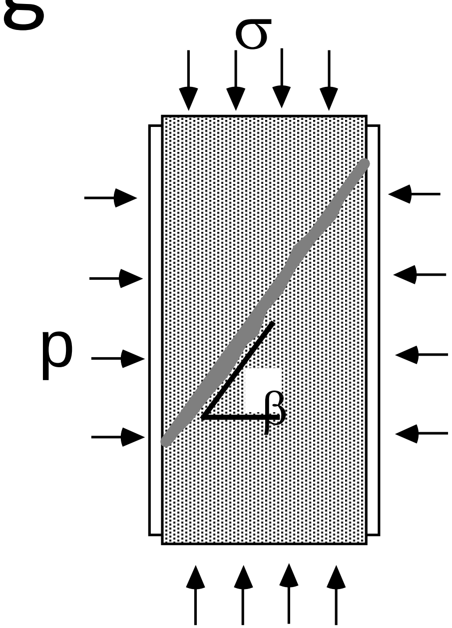

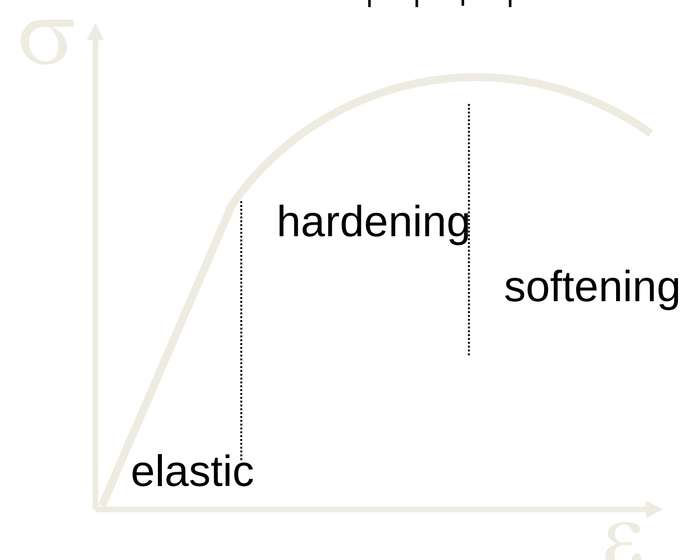

Where the Scale effect is important?

- Mathematical modelling of stability of small holes
- Interpretation of the physical experiments on small holes used to assess the stability of regular (large holes)
  - Elasticity was blamed for failure to predict the hollow cylinder strength

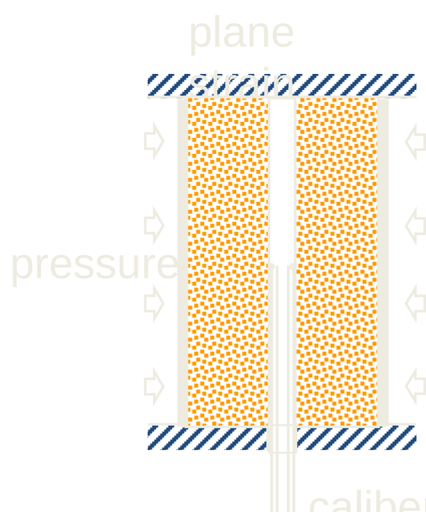

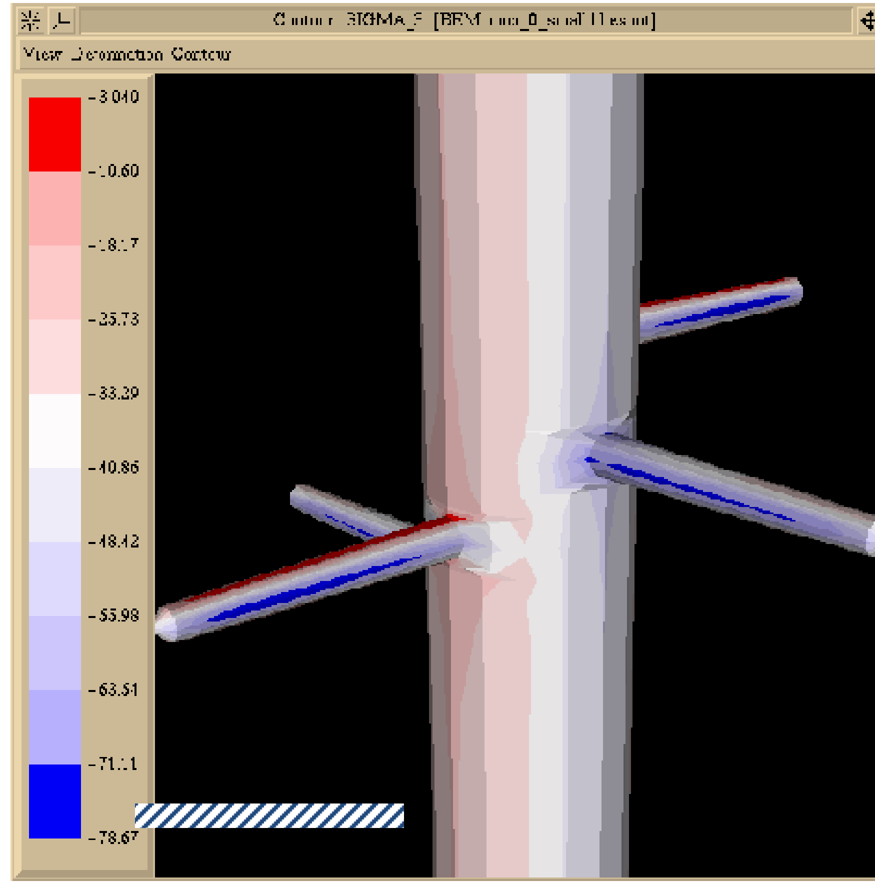

Introduction
Motivation
The problem
One way out
Outline of the talk
A Gradient Plasticity
Gradient Elastoplasticity
Outlook

How bad can it be?

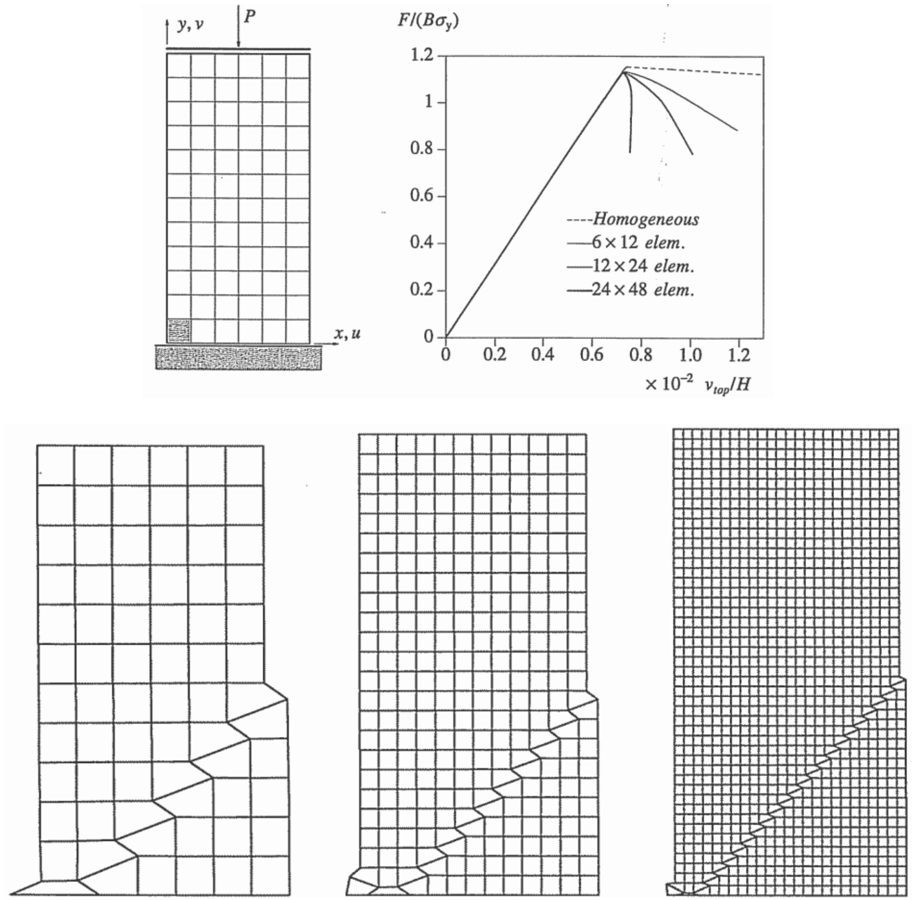

Figures from: J. Pamin, Gradient-dependent plasticity in numerical simulation of localisation phenomena.

. . . Numerical solutions are normally useless

Introduction
Motivation
The problem
One way out
Outline of the talk
A Gradient Plasticity
Gradient Elastoplasticity
Outlook

One way out

Mesh sensitivity due to lack of microstructural information.

Use a continuum theory with microstructure:

- Cosserat continuum.
  - Point rotations, as well as displacements.
- Elasticity with Microstructure (Micromorphic Elasticity).
  - Distinct kinematics of micro- and macro-volume.
- Non-local continua.
  - Stress depends on average neighbourhood strain.
- Gradient Elasticity and Gradient Plasticity.
  - Stress depends on strain gradient as well as strain.

Outline

Introduction

Cosserat Continuum

A Gradient Plasticity

Gradient Elastoplasticity

Outlook

Introduction

A Gradient Plasticity
Motivation
Equations to satisfy
Consistency condition
Solution
Example

Gradient Elastoplasticity

Outlook

Cosserat Continuum

Cosserat continuum

- Independent rotational degrees of freedom
- Non-symmetric stress tensor and couple stresses
- Extended Mohr-Coulomb flow theory of plasticity
- Parameters for Castlegate sandstone, strain softening and internal length related to grain size

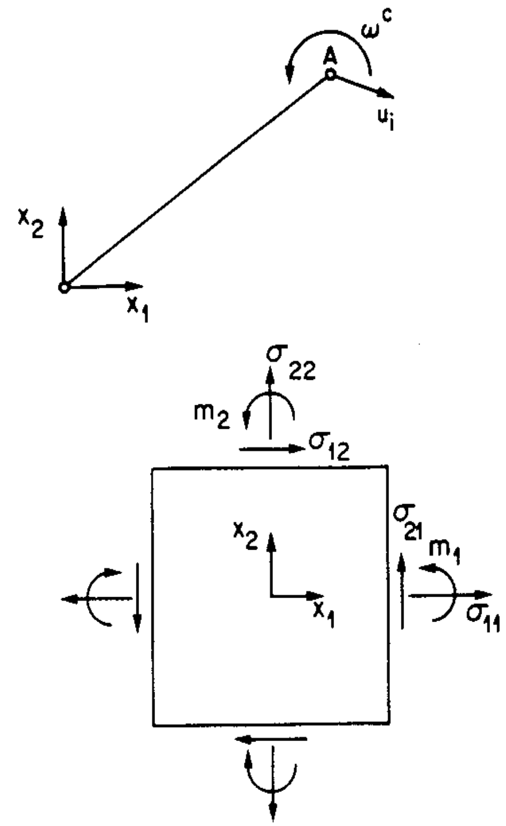

Cosserat modelling

components of the relative deformation

$$\varepsilon_{11} = u_{1,1} \qquad \varepsilon_{12} = u_{1,2} + \omega^c$$

$$\varepsilon_{21} = u_{2,1} - \omega^c \qquad \varepsilon_{22} = u_{2,2}$$

two components of curvature

$$\kappa_1 = \omega^c_{,1} \qquad \kappa_2 = \omega^c_{,2}$$

force and moment equilibrium

$$\sigma_{ij,j} = 0, \quad m_{k,k} + \sigma_{21} - \sigma_{12} = 0 \quad in \quad V$$

$$\sigma_{ij} n_j = t_i, \quad m_i n_i = m \quad on \quad \partial V$$

incremental strains

$$\varepsilon_{ij} = \varepsilon^e_{ij} + \varepsilon^p_{ij}$$

elastic strain and stress increment

$$d\varepsilon_{ij}^{e} = \left\{ 2\left(h_1 \delta_{ik}\delta_{j\ell} + h_2 \delta_{jk}\delta_{i\ell} \right) - \frac{k-1}{2k} \delta_{ij}\delta_{k\ell} \right\} \frac{d\sigma_{kl}}{2G} \qquad d\kappa_i^{e} = h_3 \frac{dm_i}{GR^2}$$

$\kappa = K/G = 1/(1\text{-}2\nu)$

Mohr–Coulomb yield criterion

$$F = \frac{\tau}{p_0 + p} - \mu = 0$$

$$\mu = \mu(\gamma^p)$$

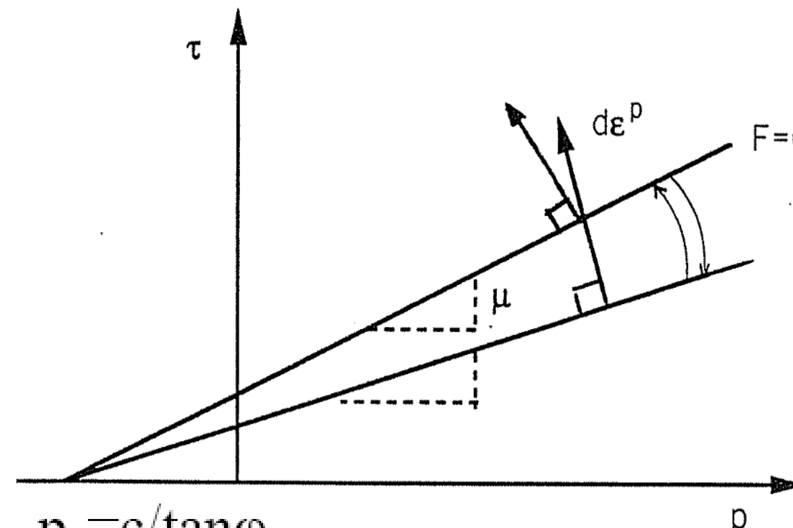

p_0=c/tanφ

Muhlhaus and Vardoulakis (1987)

$$p = \frac{\sigma_{kk}}{2} \qquad \tau = \sqrt{\left(3 s_{ij} s_{ij} - s_{ij} s_{ji}\right)/4 + m_i m_i / R^2}$$

$s_{ij=}\ \sigma_{ij} + p\delta_{ij}$

$$\gamma^p = \int d\gamma^p \qquad d\gamma^p = \sqrt{\left(3 d\varepsilon_{ij}^{p} \varepsilon_{ij}^{p} + \varepsilon_{ij}^{p} \varepsilon_{ji}^{p}\right)/2 + R^2 d\kappa_i^{p} d\kappa_i^{p}}$$

plastic potential

$$Q = \frac{\tau}{p_0 + p} - \beta \qquad \beta = \beta(\gamma^p)$$

flow-rule

$$d\varepsilon_{ij}^p = d\gamma^p \frac{\partial Q}{\partial \sigma_{ij}}$$

Finite element formulation of Cosserat model

the principle of virtual work

$$\int_V \{\delta\varepsilon\}^T \{\sigma\} dV = \int_{\partial V} \{\delta u\}^T \{t\} dS$$

$$\{u\}^T = \{u_1, u_2, \omega^c\} \qquad \{\varepsilon\}^T = \{\varepsilon_{11}, \varepsilon_{22}, \varepsilon_{12}, \varepsilon_{21}, \kappa_1 R, \kappa_2 R\}$$

$$\{\sigma\}^T = \{\sigma_{11}, \sigma_{22}, \sigma_{12}, \sigma_{21}, m_1 / R, m_2 / R\} \qquad \{t\}^T = \{t_1, t_2, m\}$$

elastic and plastic parts

$$\{d\varepsilon\} = \{d\varepsilon^e\} + \{d\varepsilon^p\}$$

elastic strain and stress increment

$$\{d\sigma\} = \left[D^e\right]\{d\varepsilon^e\}$$

matrix $[D^e]$ contains the elastic parameters of a two dimensional, linear-elastic, isotropic Cosserat continuum defined by

$$\left[D^e\right] = \begin{bmatrix} K+G & K-G & 0 & 0 & 0 & 0 \\ K-G & K+G & 0 & 0 & 0 & 0 \\ 0 & 0 & G+G^c & G-G^c & 0 & 0 \\ 0 & 0 & G-G^c & G+G^c & 0 & 0 \\ 0 & 0 & 0 & 0 & M & 0 \\ 0 & 0 & 0 & 0 & 0 & M \end{bmatrix}$$

so-called static Cosserat model Muhlhaus and Vardoulakis (1987) proposed

$$\frac{G^C}{G} = \frac{1}{2}, \qquad \frac{M}{G} = R^2$$

plastic strain and plastic curvature increments

$$\left\{ d\varepsilon^p \right\} = d\gamma^p \left\{ \frac{\partial Q}{\partial \sigma} \right\}$$

Prager's consistency condition, $F = 0$ and $dF = 0$;

$$d\gamma^p = \frac{\left\{ \frac{\partial F}{\partial \sigma} \right\} \left(\left[D^e \right] \left\{ d\varepsilon \right\} \right)}{\left\{ \frac{\partial F}{\partial \sigma} \right\} \cdot \left(\left[D^e \right] \left\{ \frac{\partial Q}{\partial \sigma} \right\} \right) + \left(p_0 + p \right) h_t}$$

plastic modulus

$$h_t = d\mu \,/\, d\gamma^p$$

stress increment

$$\{d\sigma\} = \left[D^{ep}\right]\{d\varepsilon\}$$

stiffness matrix

$$\left[D^{ep}\right] = \left[D^{e}\right] - \langle 1 \rangle \frac{\left(\left[D^{e}\right]\left\{\frac{\partial Q}{\partial \sigma}\right\}\right) \cdot \left(\left[D^{e}\right]\left\{\frac{\partial F}{\partial \sigma}\right\}\right)^{T}}{\left\{\frac{\partial F}{\partial \sigma}\right\}\left(\left[D^{e}\right]\left\{\frac{\partial Q}{\partial \sigma}\right\}\right) + \left(p_0 + p\right)h}$$

Loading of the yield surface F = 0 takes place when $d\gamma^{p}>0$

$$\langle 1 \rangle = \begin{cases} 1 \quad if \quad F = 0 \quad and \quad d\gamma^{p} > 0 \\ 0 \quad if \quad F < 0 \quad or \quad \left\{F = 0 \quad and \quad d\gamma^{p} \leq 0\right\} \end{cases}$$

Material parameters (hardening-softening)

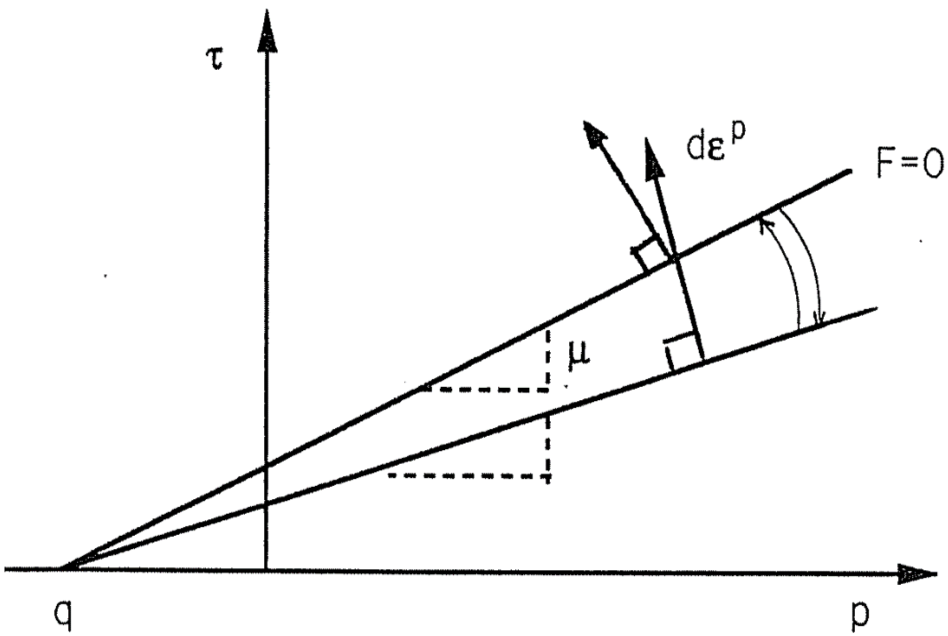

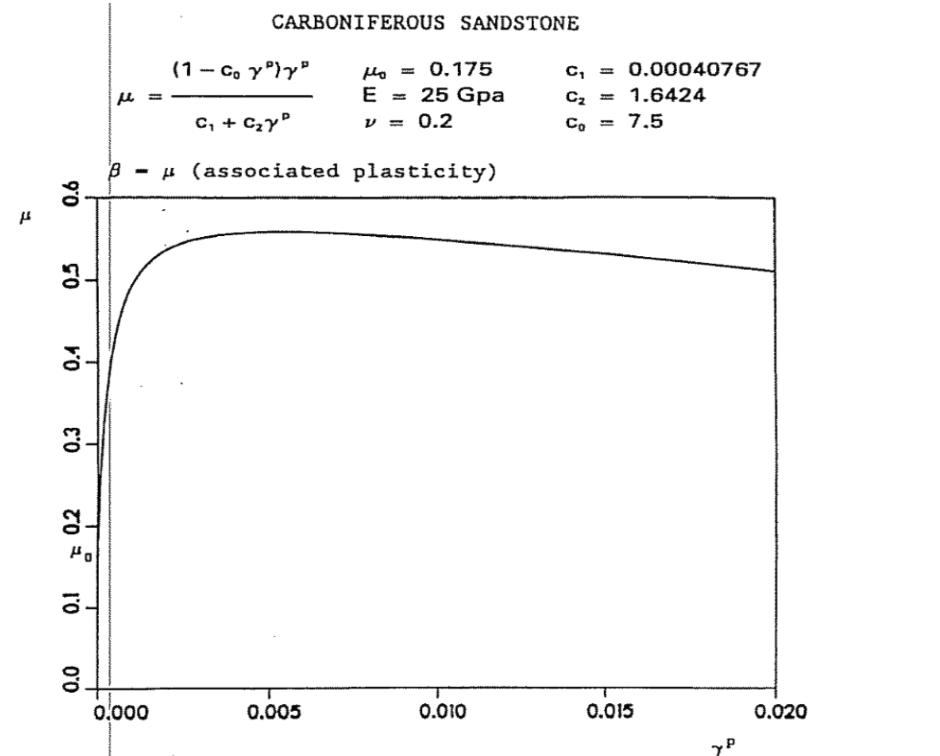

Mobilized friction coefficient versus accumulated plastic shear strain for a 'Carboniferous sandstone'.

$E = 25$ GPa and Poisson's ratio, $\nu = 0{\cdot}2$.

$\mu = \mu_o + \mu_1$

$$\mu_1 = \frac{(1 - c_0\gamma^p)\gamma^p}{c_1 + c_2\gamma^p}$$

Finite Elements Implementation

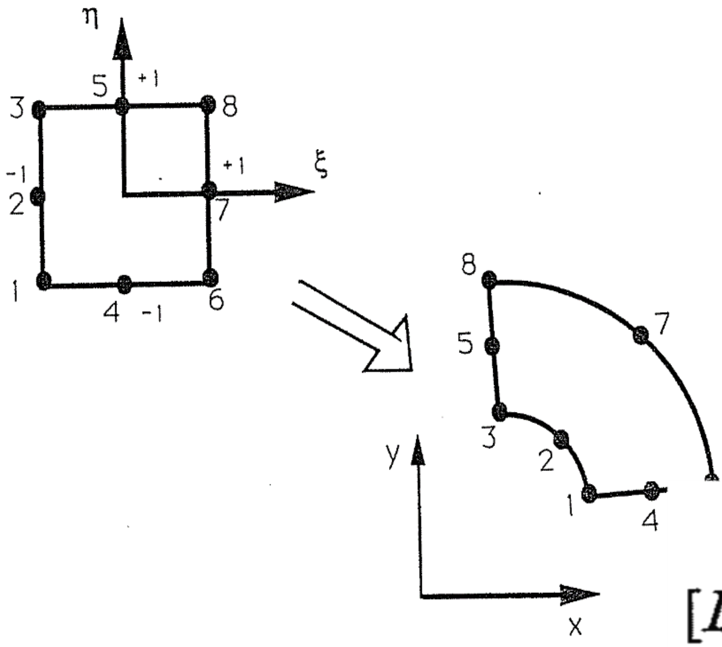

$$\{u\} = [N]\{U\}$$

$$\{\Delta\epsilon\} = [B]\{\Delta U\}$$

$$[B] = [L][N]$$

$$[L]^T = \left| \begin{matrix} \frac{\partial}{\partial x} & 0 & \frac{\partial}{\partial y} & 0 & 0 & 0 \\ 0 & \frac{\partial}{\partial y} & 0 & \frac{\partial}{\partial x} & 0 & 0 \\ 0 & 0 & 1 & -1 & R\frac{\partial}{\partial x} & R\frac{\partial}{\partial y} \end{matrix} \right.$$

$$x(\xi,\eta) = \sum_{i=1}^{8} x_i \, N_i(\xi,\eta)$$

$$y(\xi,\eta) = \sum_{i=1}^{8} y_i \, N_i(\xi,\eta)$$

$N_1(\xi,\eta)=-0.25(1-\xi)(1-\eta)(1+\xi+\eta)$

$N_2(\xi,\eta)=0.5(1-\xi^2)(1-\eta)$

$N_3(\xi,\eta)=0.25(1+\xi)(1-\eta)(\xi-\eta-1)$

$N_4(\xi,\eta)=0.5(1+\xi)(1-\eta^2)$

$N_5(\xi,\eta)=0.25(1+\xi)(1+\eta)(\xi+\eta-1)$

$N_6(\xi,\eta)=0.5(1-\xi^2)(1+\eta)$

$N_7(\xi,\eta)=0.25(1-\xi)(1+\eta)(-\xi+\eta-1)$

$N_8(\xi,\eta)=0.5(1-\xi)(1-\eta^2)$

$$\{\epsilon\} = [L]\{u\}$$

Plasticity integration algorithm

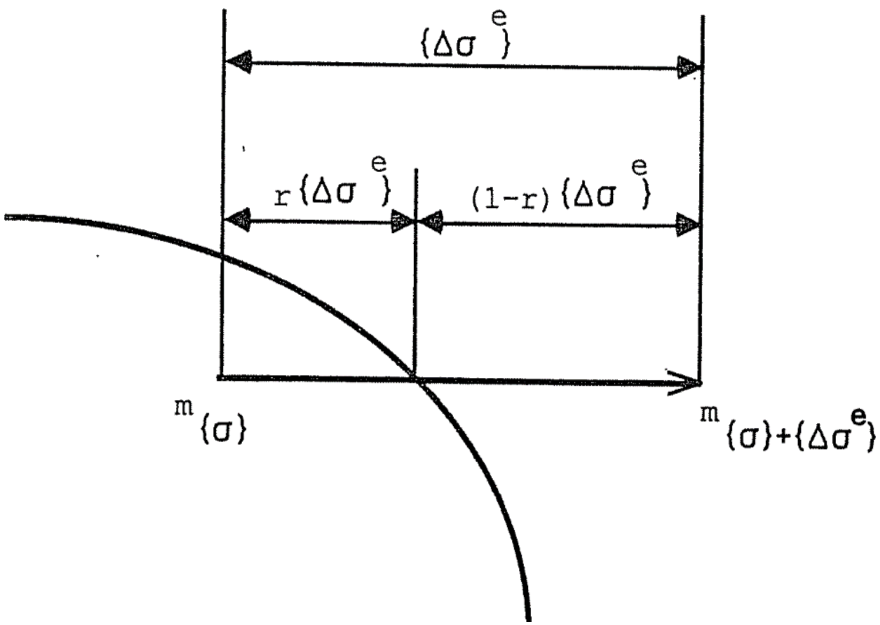

$$r = \frac{-F(^m\{\sigma\}, {}^m\gamma^p)}{\left\{\frac{\partial F}{\partial\{\sigma\}}\right\}^T \Big|_{^m\{\sigma\}} \{\Delta\sigma^e\}}$$

elastic to plastic state

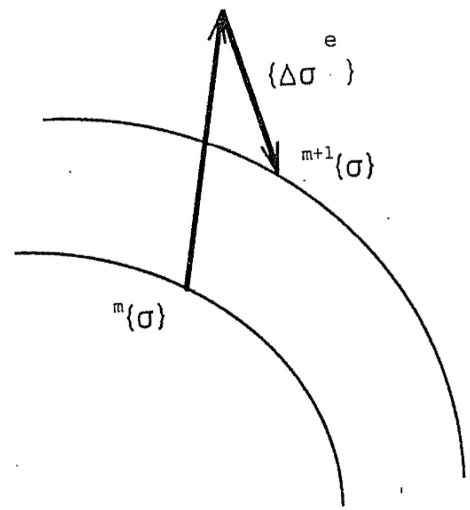

Return mapping

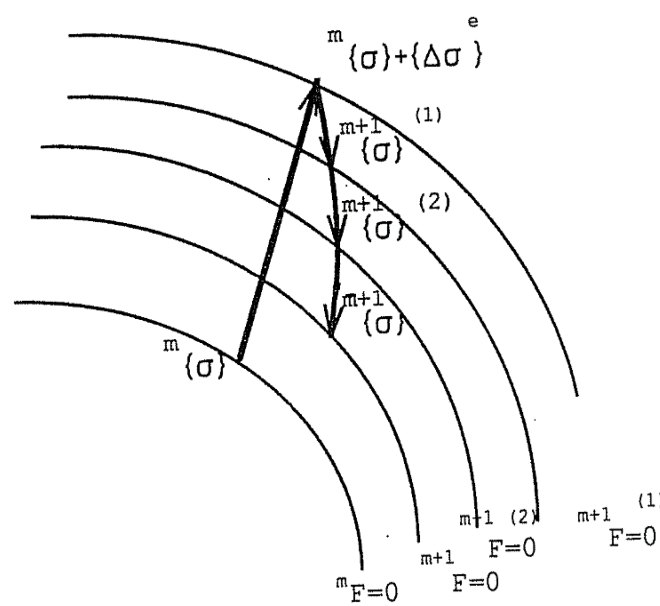

Continuation Methods

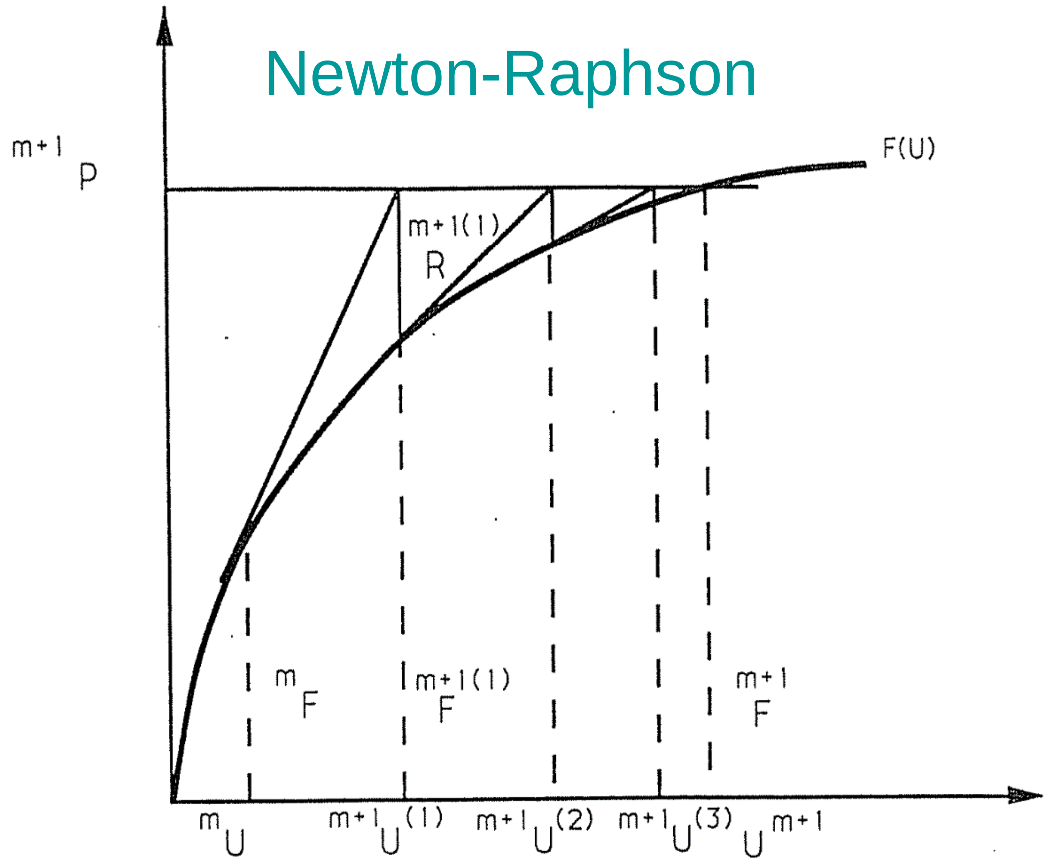

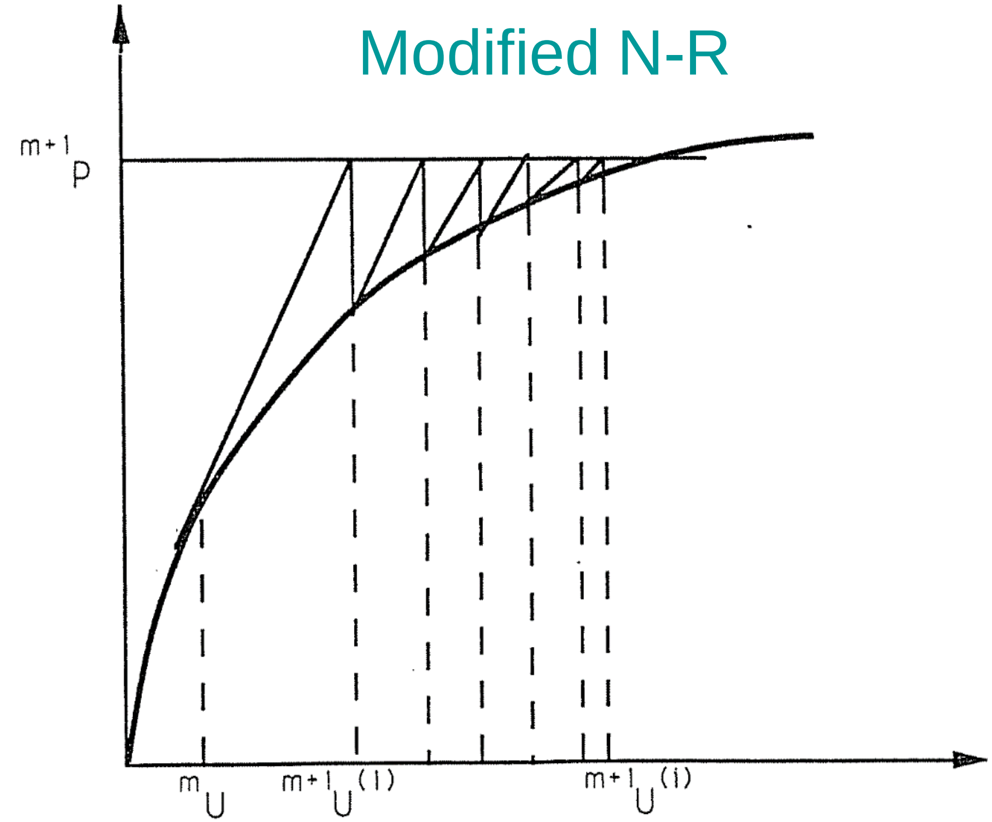

$$\int_V [B]^T [D^{ep}][B]\{\Delta U\} dV = \lambda_{m+1}\{P\} - \int_V [B]^T\{\sigma_m\} dV$$

$$[K] = \int_V [B]^T [D^{ep}][B] dV \qquad \{R\} = \lambda_{m+1}\{P\} - \int_V [B]^T\{\sigma_m\} dV$$

$$[K]\{\Delta U\} = \{R\}$$

Arc-Length Method

Displacement Control

$$\{\Delta U\}^{(j)} = \Delta\lambda^{(j)}\{\Delta U\}_{\mathrm{I}}^{(j)} + \{\Delta U\}_{\mathrm{II}}^{(j)}$$

$$\{\Delta U\}_{\mathrm{I}}^{(j)} = [K^{(i)}]^{-1}\{P\}$$

$$\{\Delta U\}_{\mathrm{II}}^{(j)} = [K^{(i)}]^{-1}\{R\}^{(i)}$$

$$\lambda_{m+1}^{(j)} = \lambda_{m+1}^{(i)} + \Delta\lambda^{(j)}$$

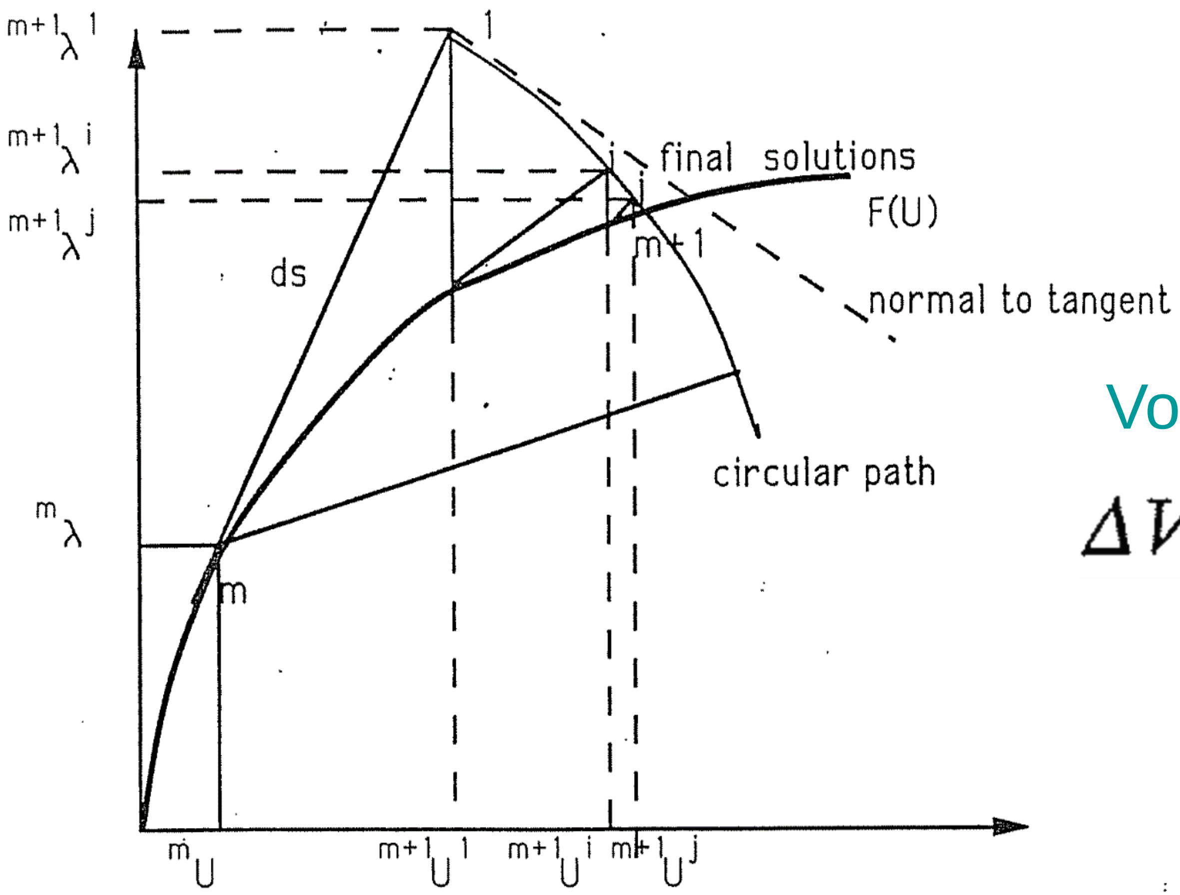

Volume control

$$\Delta V^{(j)} = \Delta\lambda^{(j)}\,\Delta V_{\mathrm{I}}^{(j)} + \Delta V_{\mathrm{II}}^{(j)}$$

$$\Delta\lambda^{(1)} = \frac{\Delta V - \Delta V_{\mathrm{II}}^{(1)}}{\Delta V_{\mathrm{I}}^{(1)}}$$

$$\Delta\lambda^{(j)} = -\frac{\Delta V_{\mathrm{II}}^{(j)}}{\Delta V_{\mathrm{I}}^{(j)}}$$

Softening in classical plasticity

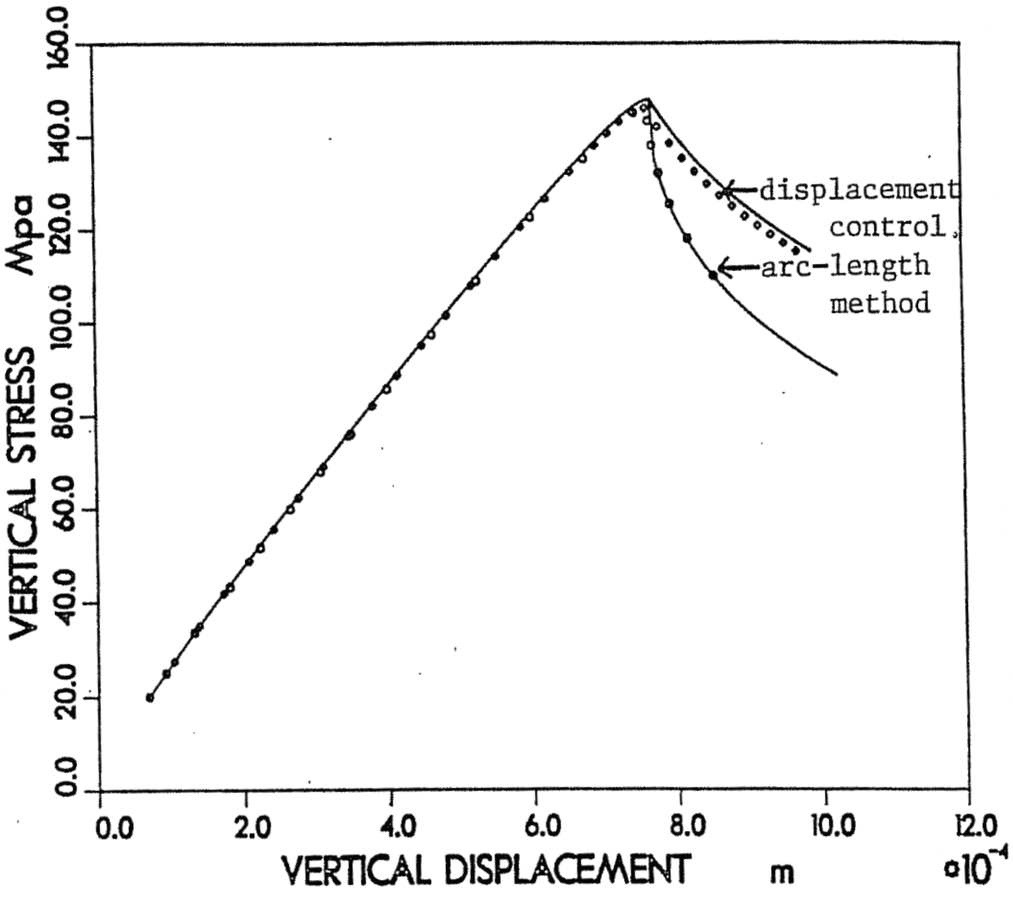

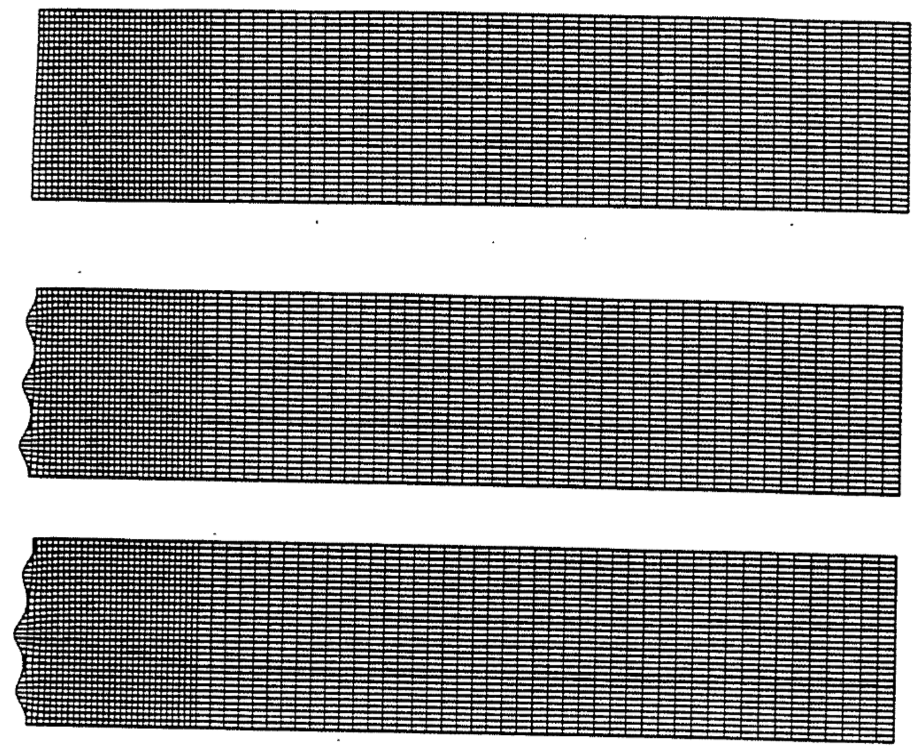

Borehole Failure

- failure in geomaterials takes place in localized deformation in shear bands

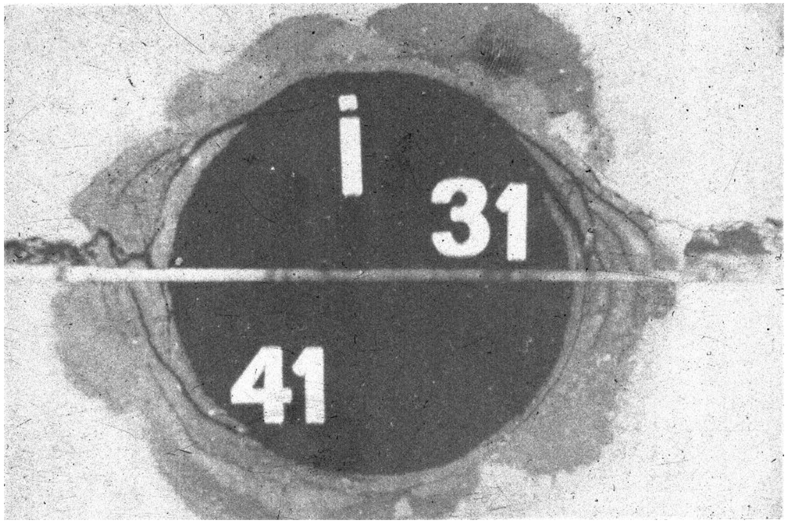

Borehole analysis

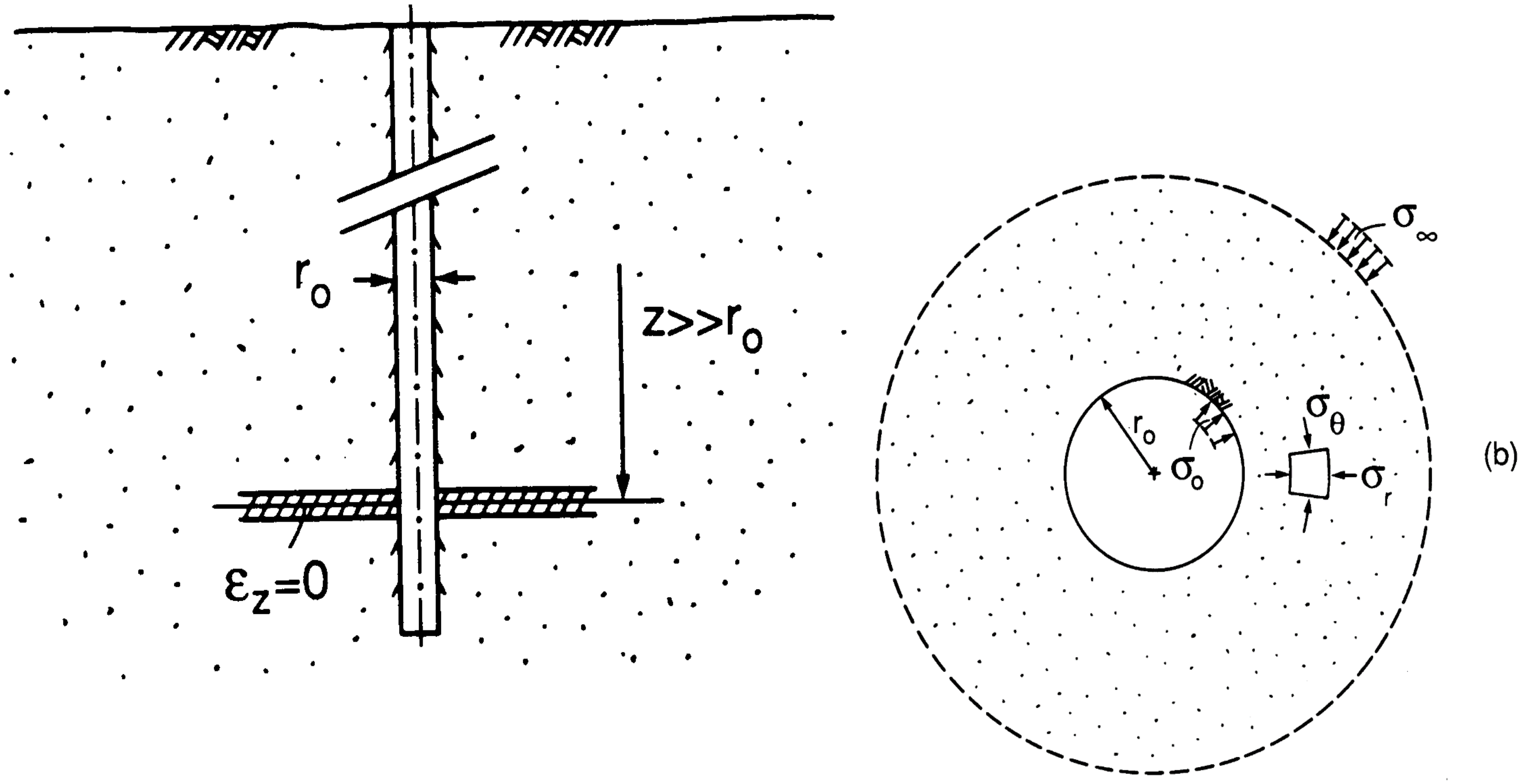

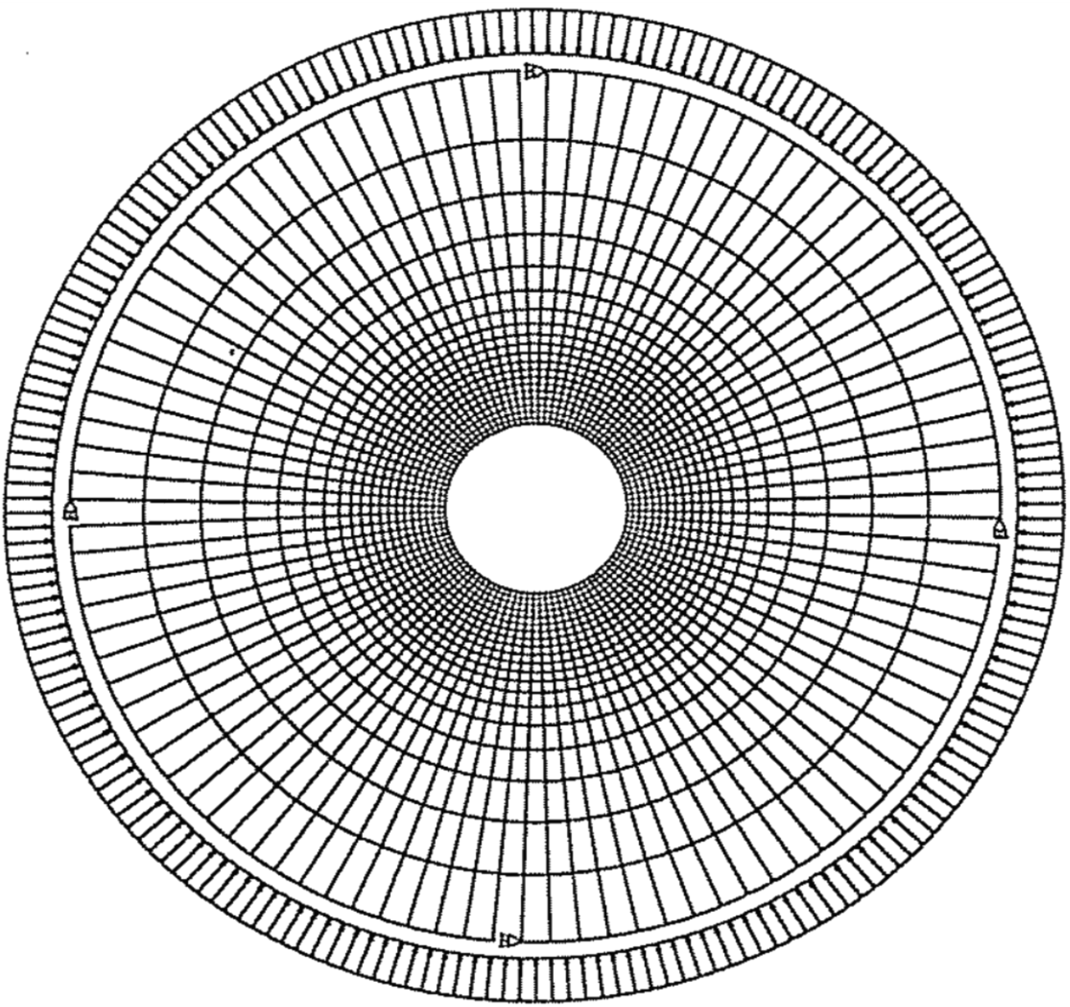

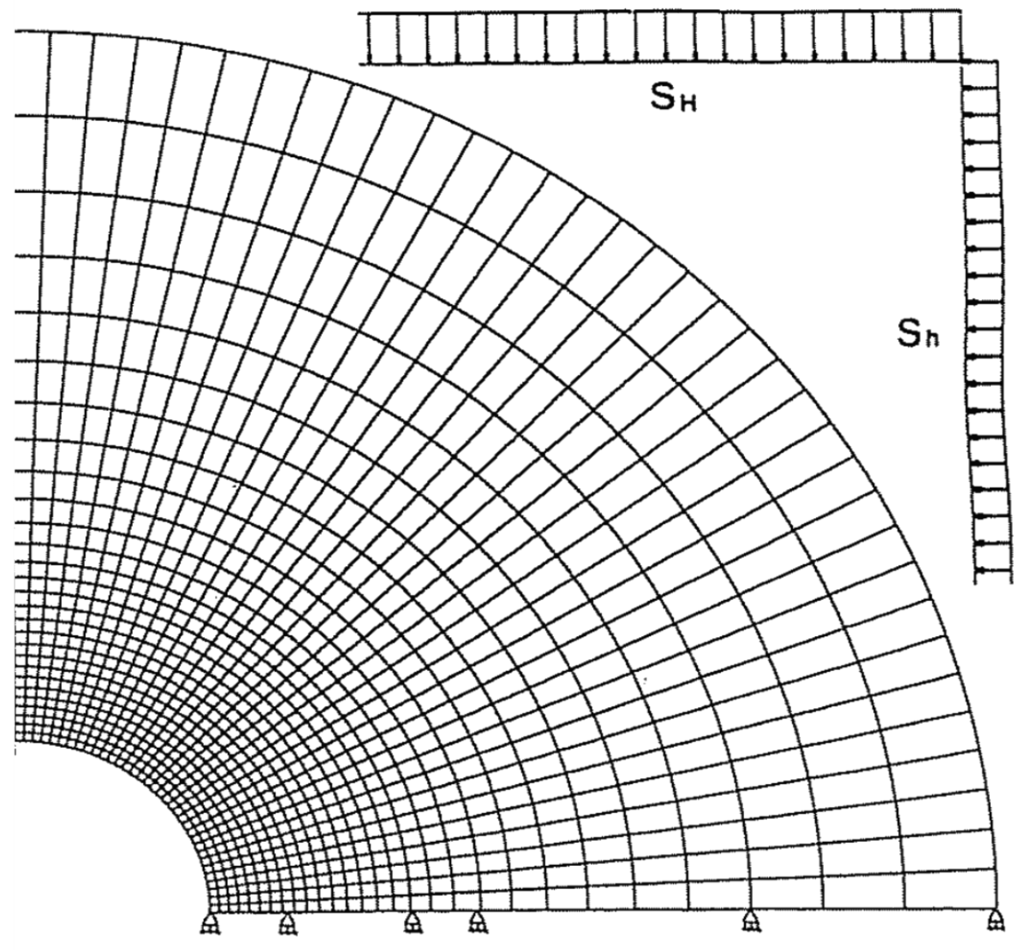

SH
Sh

Bifurcation analysis

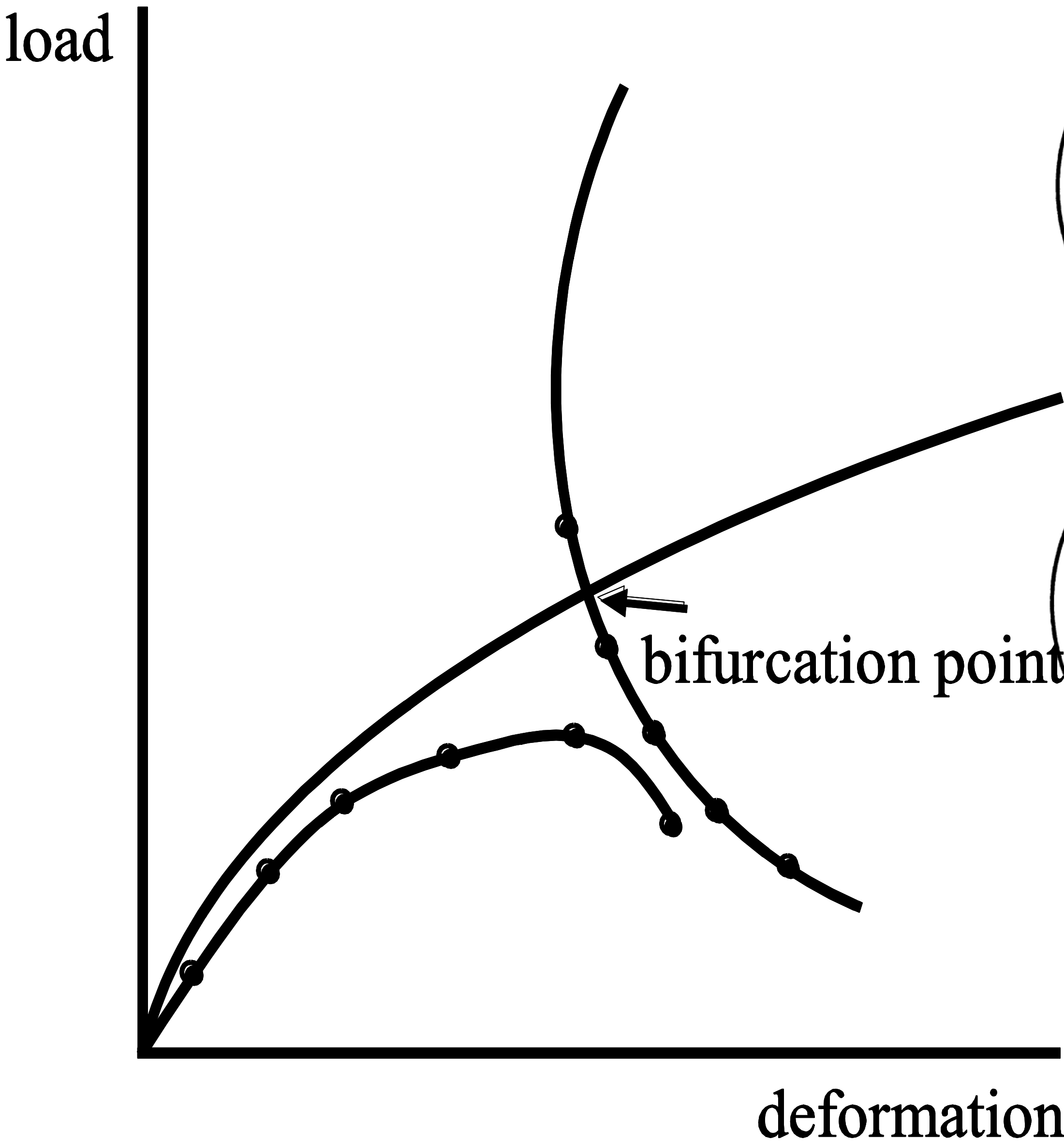

conditions for a bifurcation

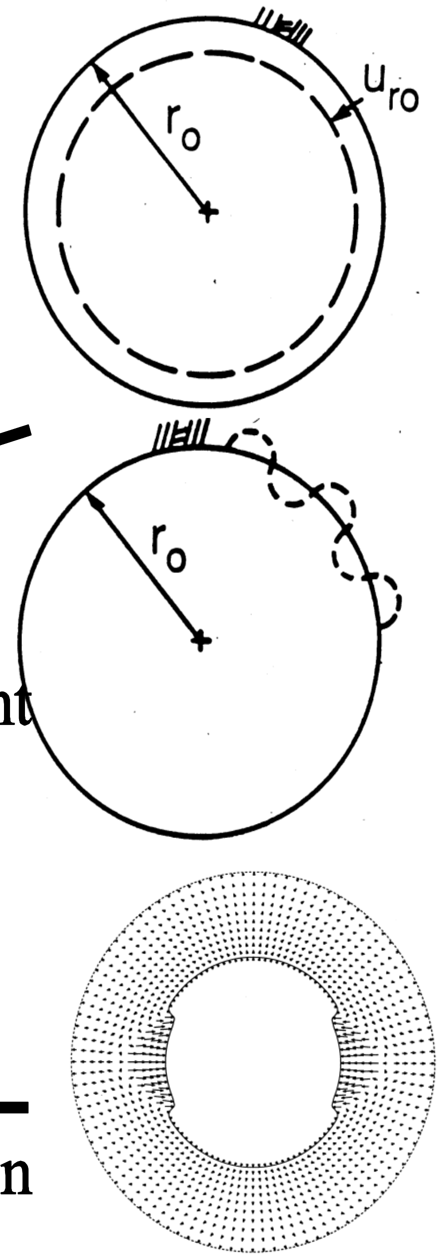

$$\int_V \Delta\sigma_{ij}\Delta\epsilon_{ij} DV = 0$$

$$det([K]) = 0$$

Eigen-value analysis

TABLE 1
Eigenvalue Analysis at Bifurcation Point (see Fig. 7)

real part	*imaginary part*	*eigenvector (wave-number)*
0·51896E-03	0·00000E+00	10
0·80039E-03	0·00000E+00	12
0·14811E-02	0·00000E+00	8
0·21925E-02	0·00000E+00	14
0·25344E-02	0·00000E+00	16

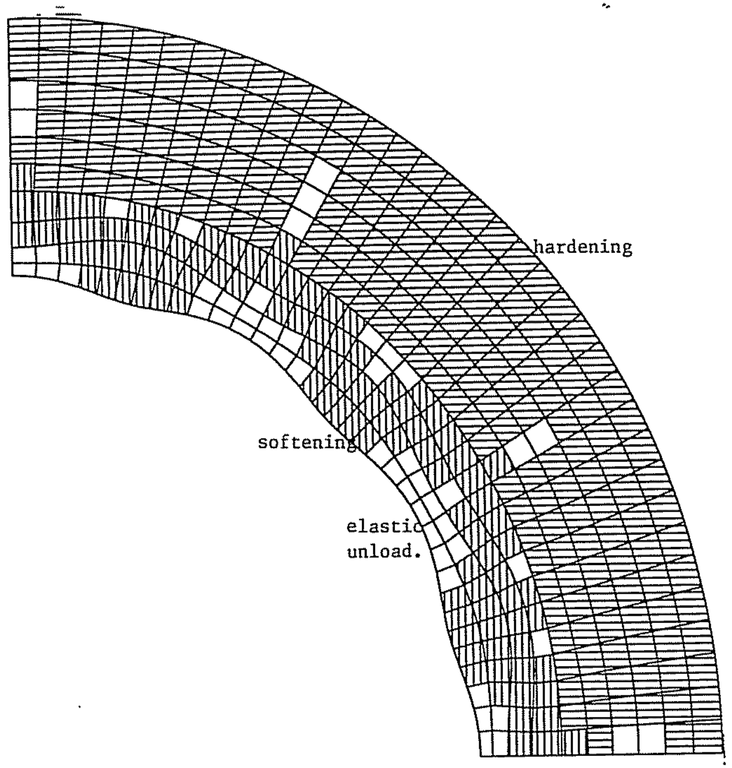

Detail of eigenvector with element state at first step of localization, warping mode $m = 12$ ($r_0 = 6$ cm, $\sigma_\infty/p_o = 2{\cdot}388$).

Papanastasiou and Vardoulakis (1992)

Isotropic stress-field

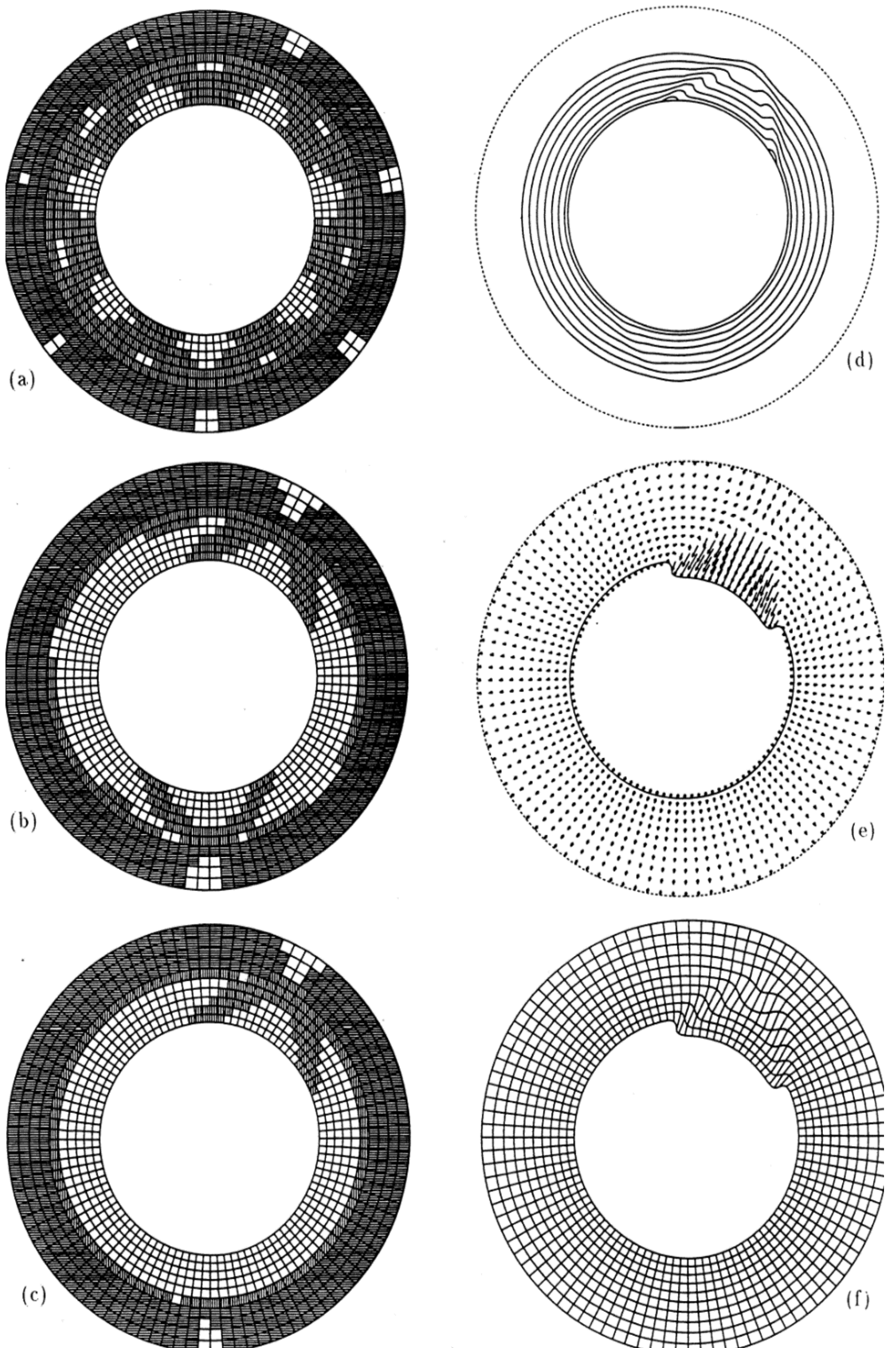

$r_0 = 3$ cm

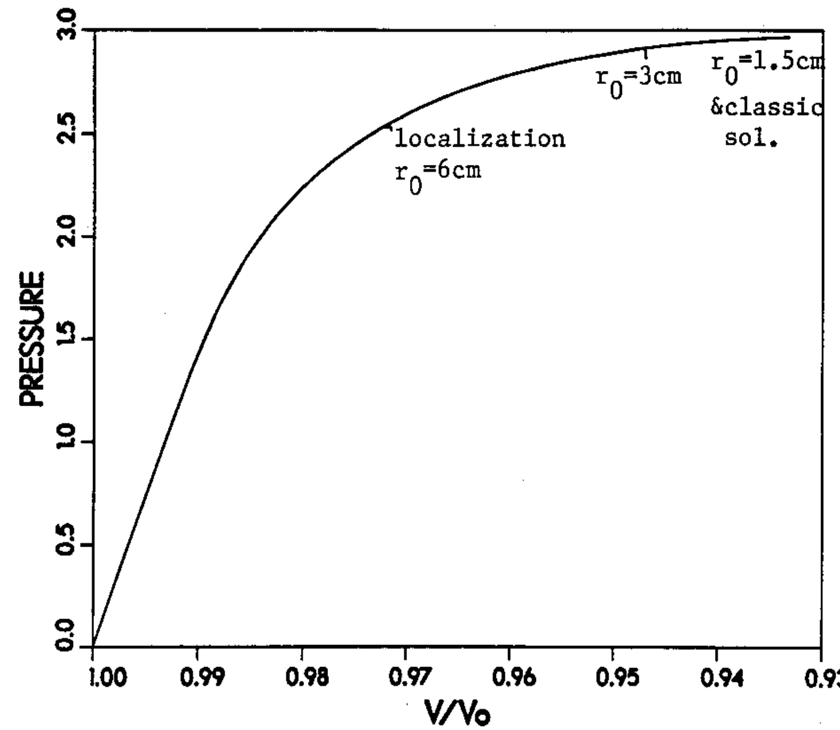

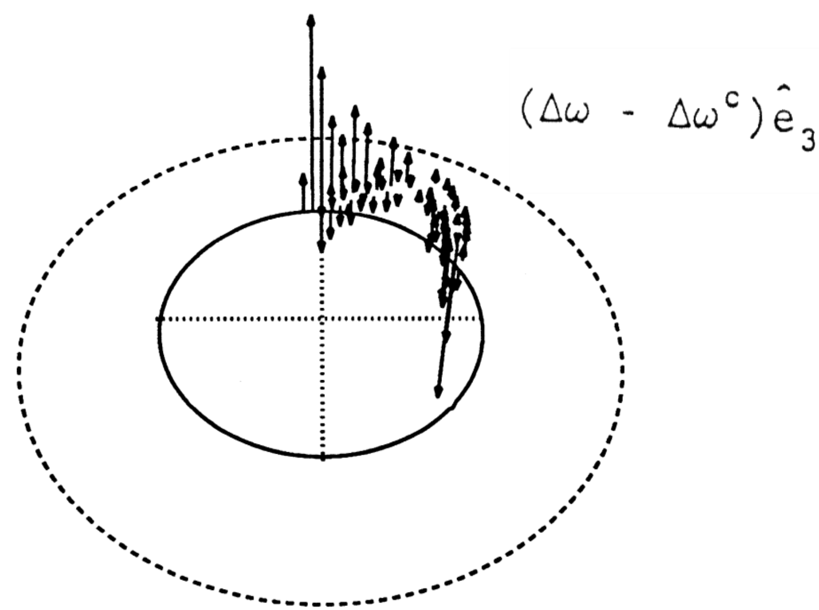

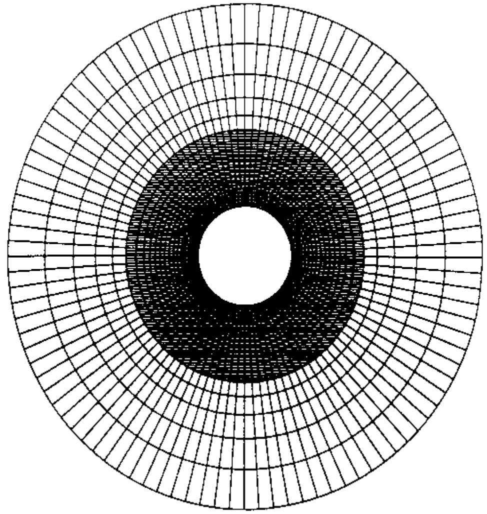

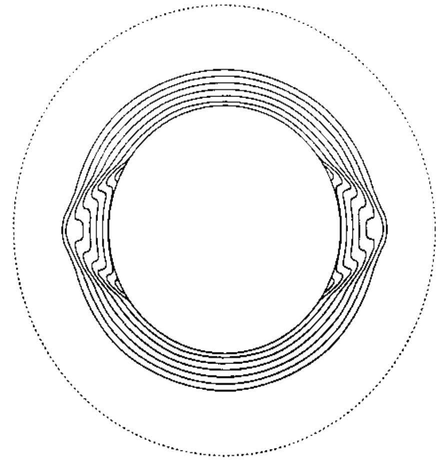

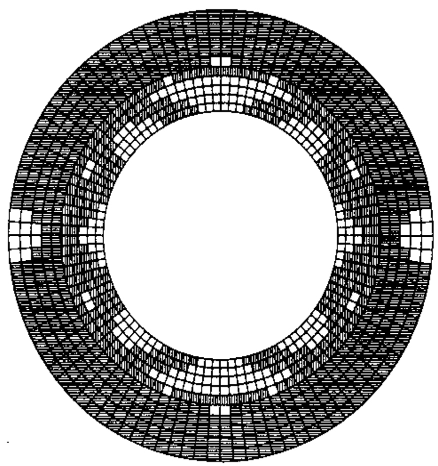

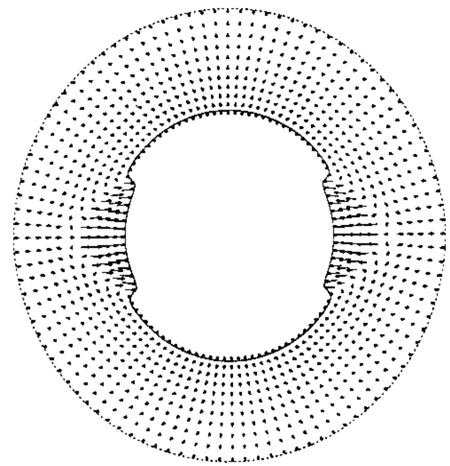

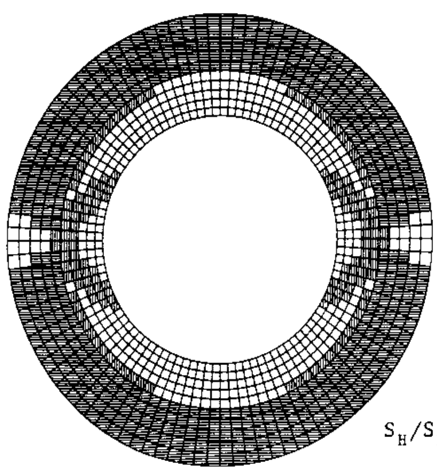

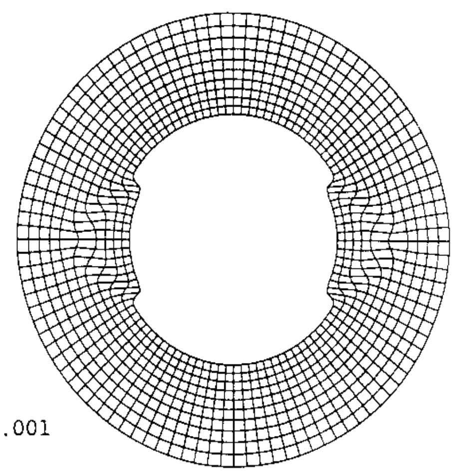

$S_H/S_h = 1.001$

$r_0 = 3$ cm

Anisotropic stress-field

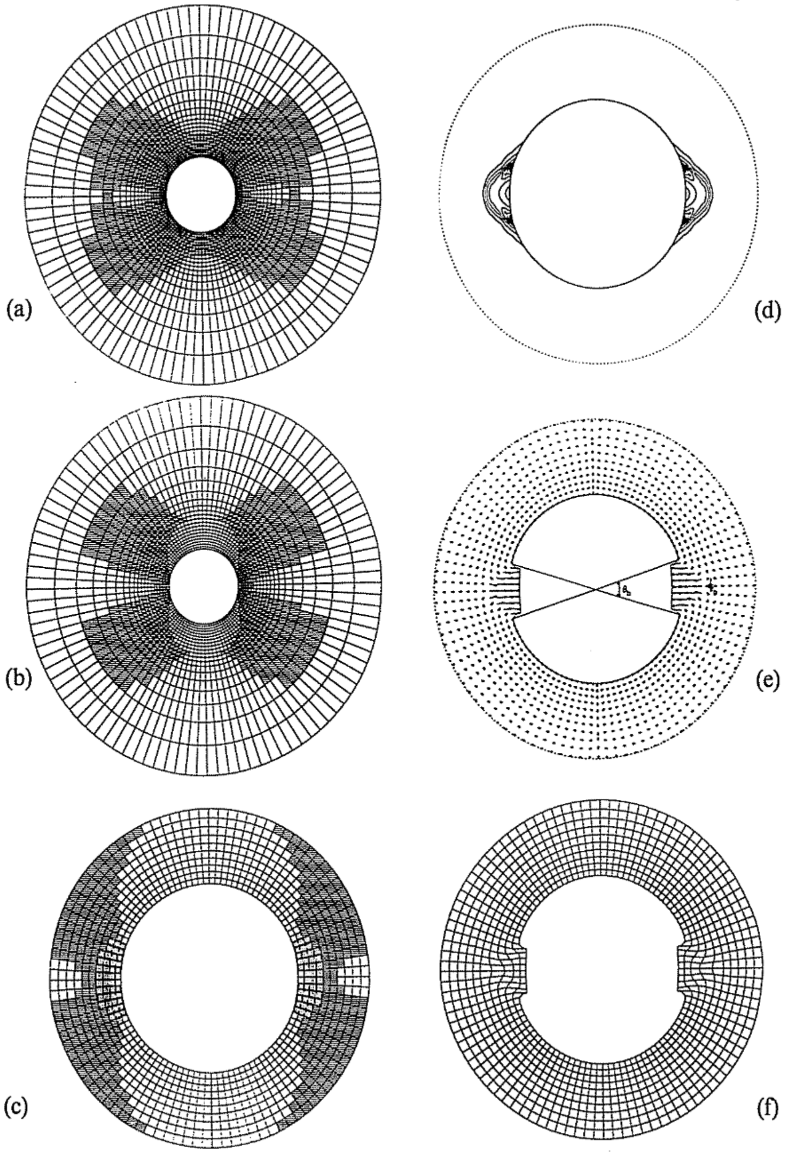

FIG. 13. Global picture of elastic-plastic domains (a) before localization, (b) after localization. Details of (c) elastic-plastic domains, (d) isolines of accumulated plastic shear strain, γ^p, (e) incremental displacement field, (f) deformed mesh, after localization (r_0 = 3 cm, S_H/p_o = 2·053, S_H/S_h = 1·5).

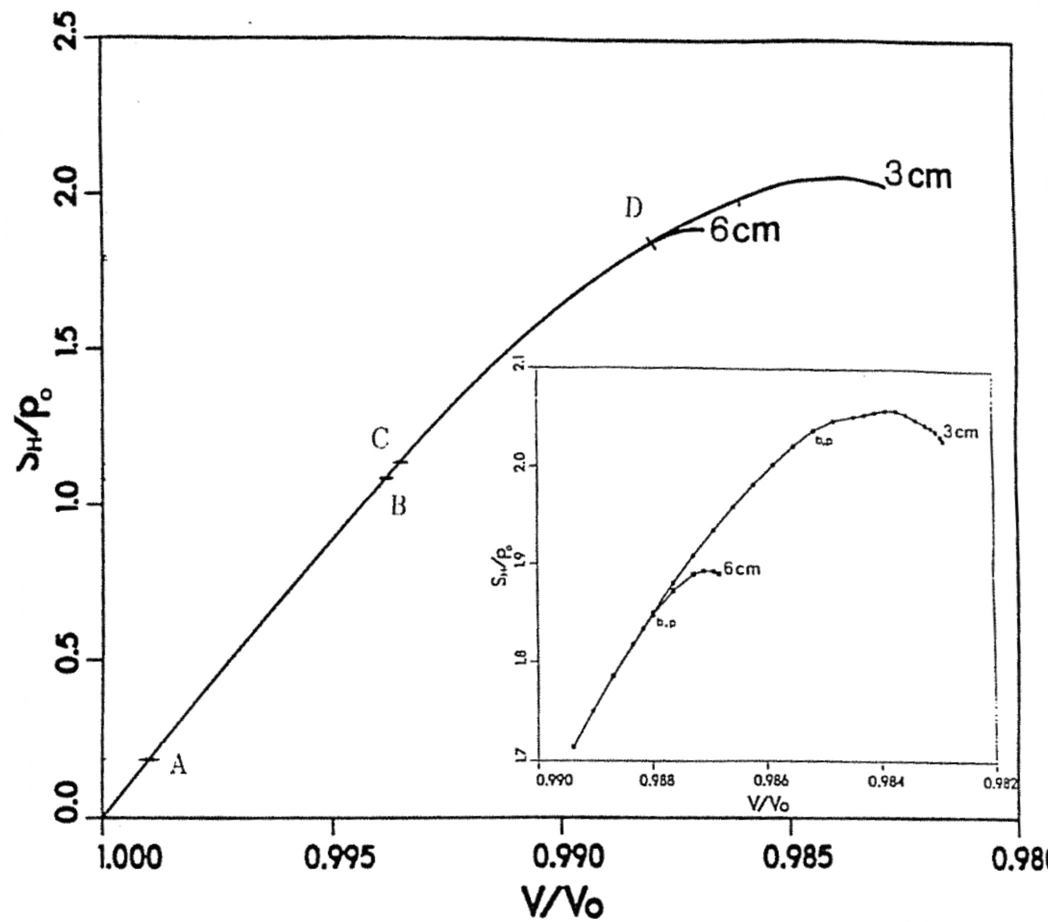

Papanastasiou and Vardoulakis, 1994

Breakouts prediction

Size of Borehole Breakouts

r_o, cm	S_H/S_h	θ°_b	r_b/r_o
3	1·0	58	1·42
3	1·5	32	1·25
6	1·5	30	1·23
6	3·0	22	1·12

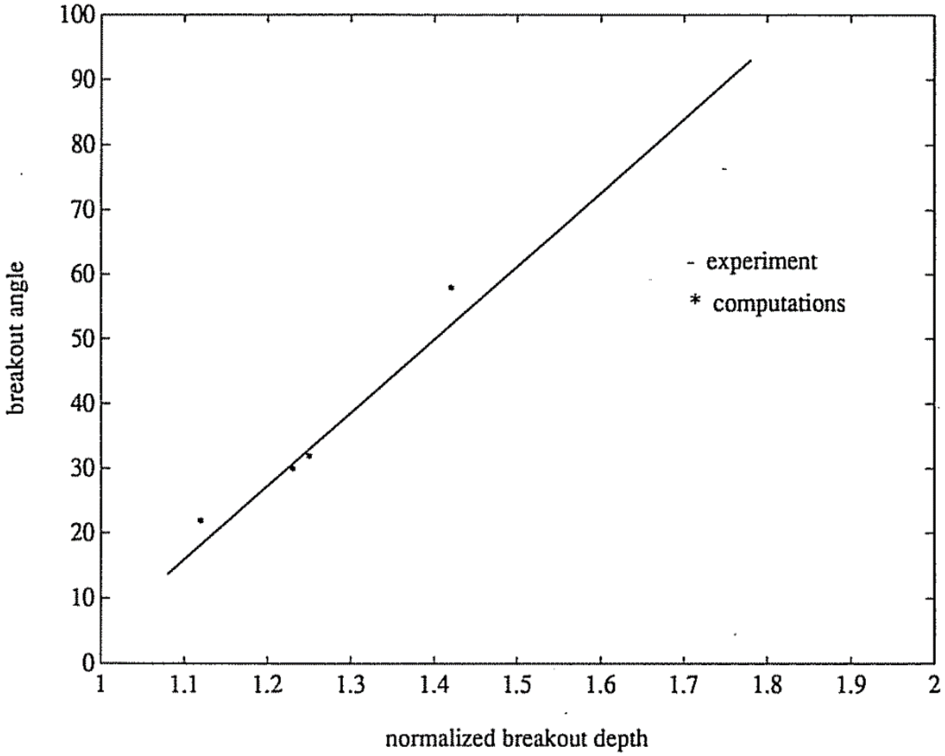

FIG. 14. Comparison of experimental and computational results.

Experimental results
Haimson and Herrick, 1989

Comparison with thick-walled cylinder test

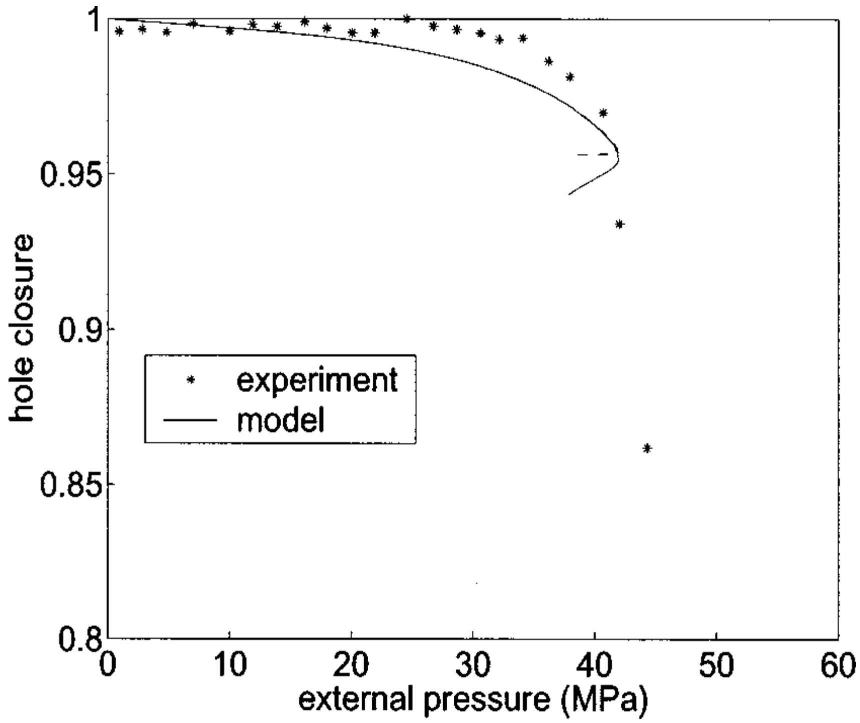

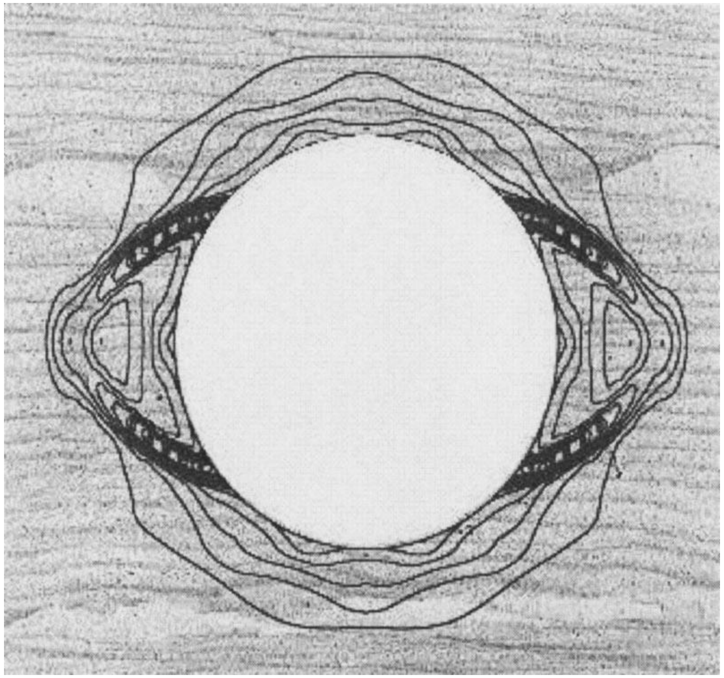

Papanastasiou and Zervos, 2000

Elliptical Shape Perforations: an engineering application based on Cosserat modelling

- Introduction
  - sand avoidance from perforated intervals
- Computational results
  - elastic analysis
  - Cosserat elastoplastic analysis
- Conclusion
  - practical application

Sand production and avoidance

- Sanding problem ($2 billion/year)
  - blocks perforations, damages of equipment, requires separation from the oil and disposal
- Avoidance
  - gravel packing and screening, preferential perforating, fracturing
- Objective
  - develop models to predict sanding and optimum completion

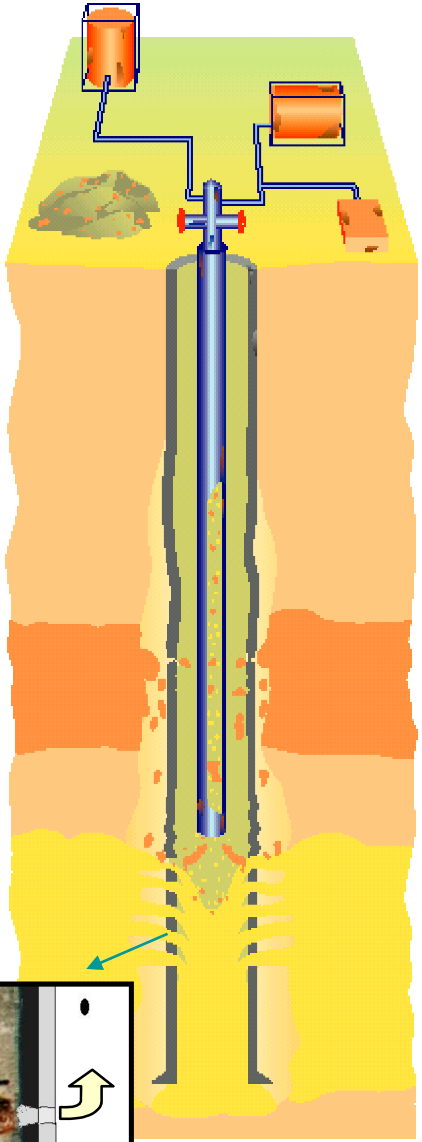

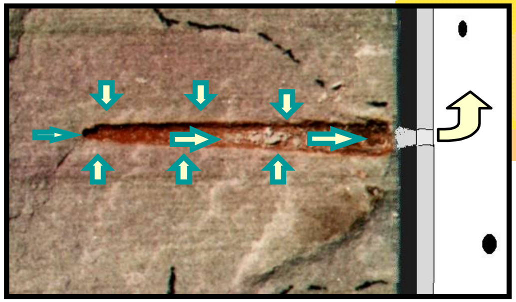

Real perforation

Mechanisms of sand production

- Hollow Cylinder Tests
  - various weak sandstones
  - 10-20 mm perforation size
  - hydrostatic pressure
- Sand production in two stages
  - stresses due to drawdown and depletion fail the rock
  - high flow velocities transport loose grain
- Unconsolidated formation
  - erosion mechanism

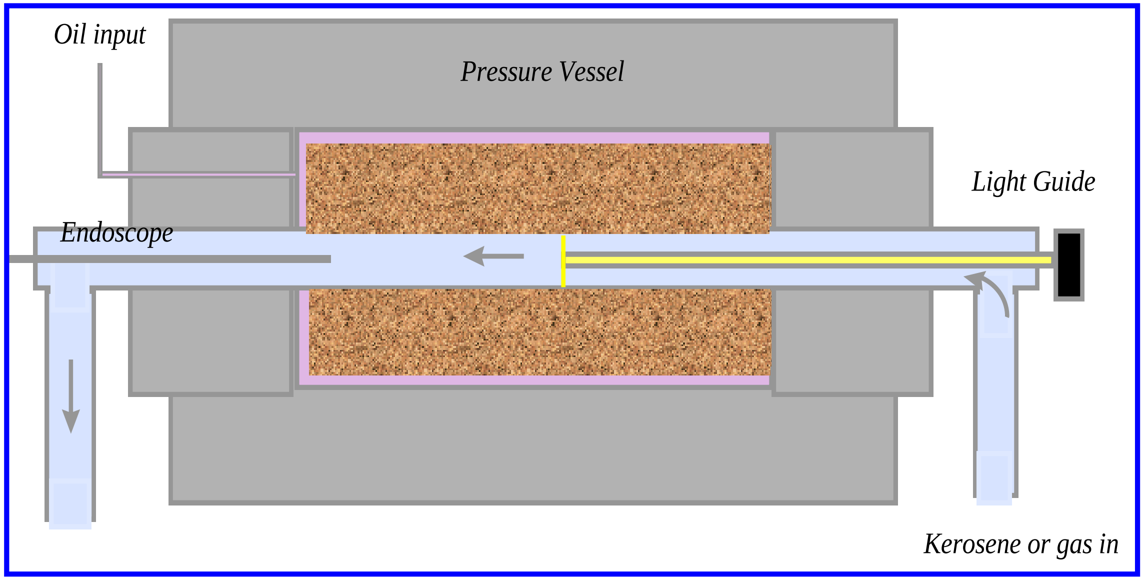

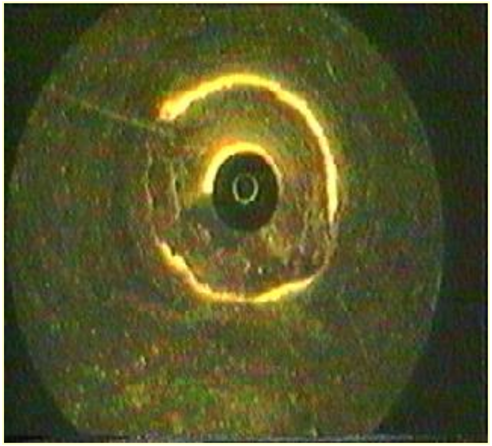

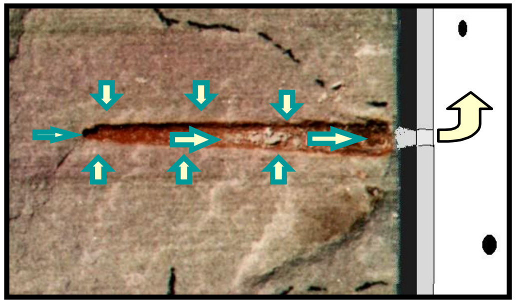

Real perforation

Cook and Nicholson (SCR)

Production from perforated intervals

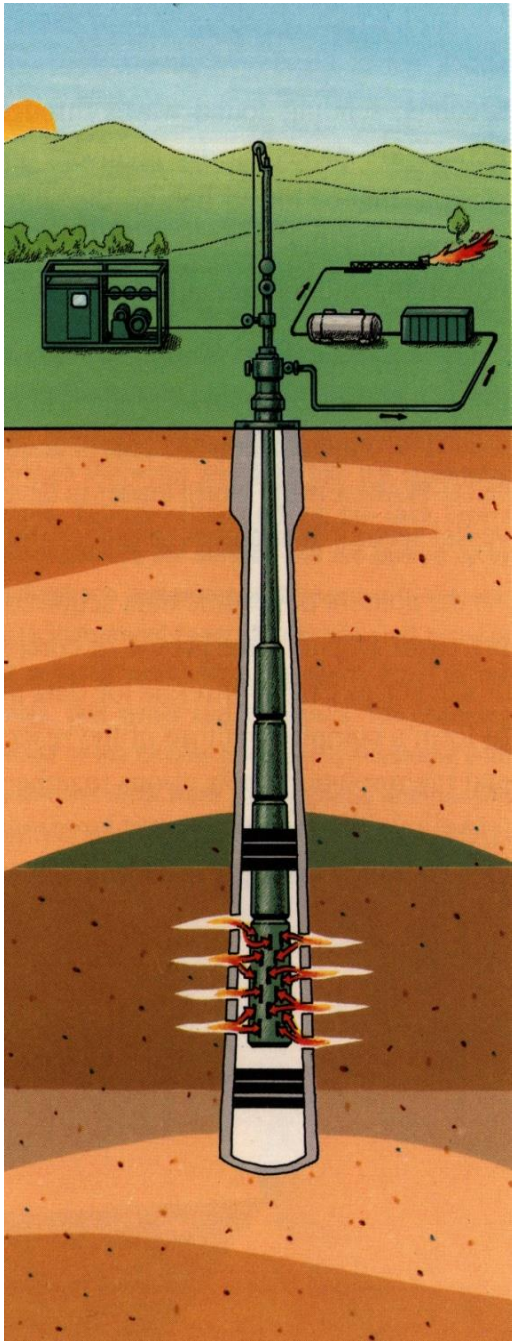

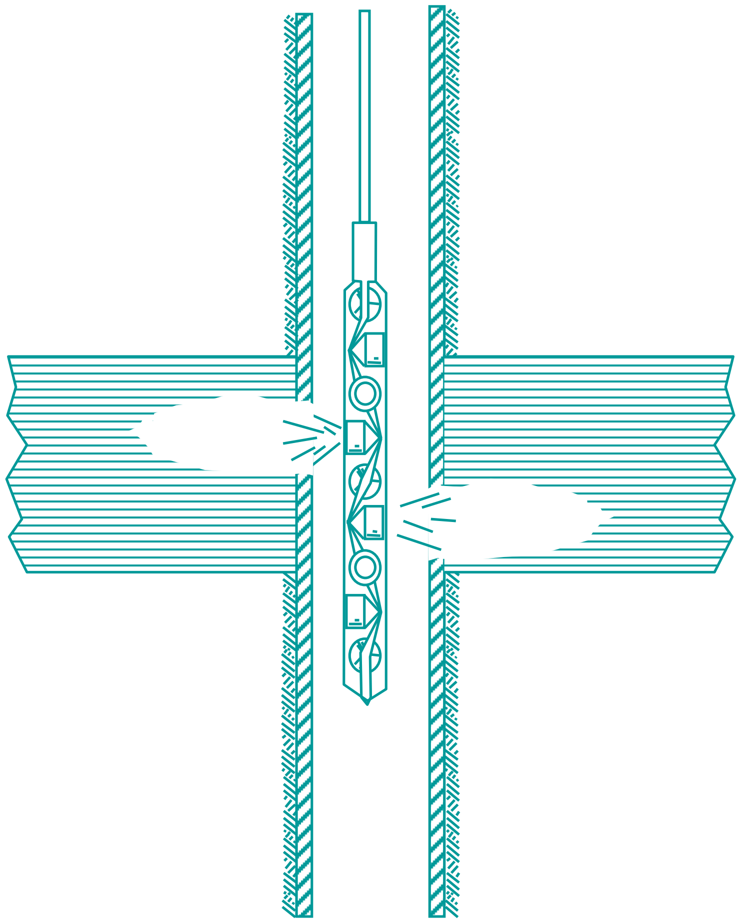

Perforating tool

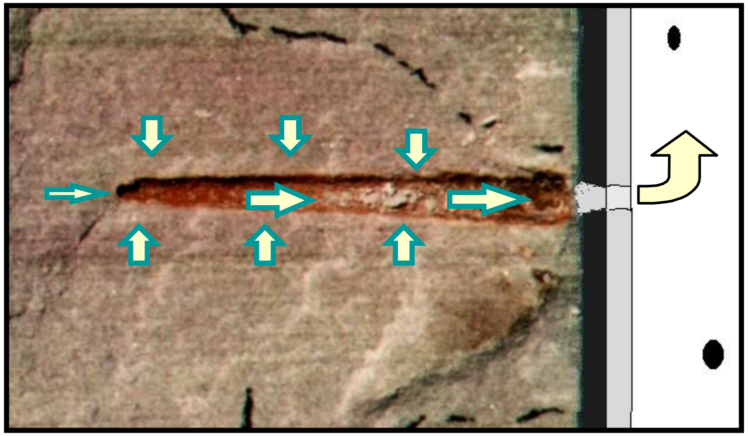

Real perforation

Sand avoidance

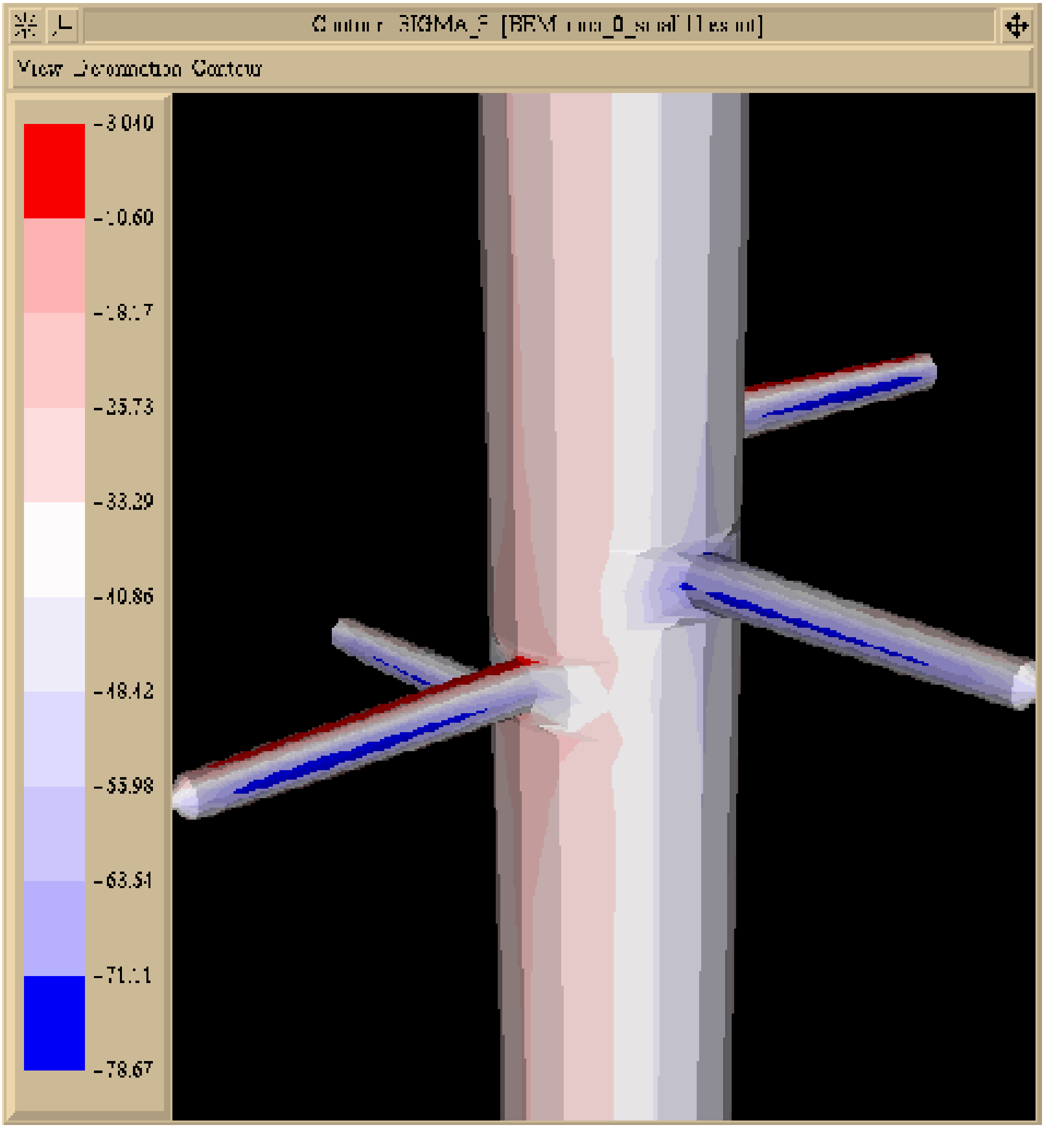

- perforation failure caused by high compressive stresses results in sand production
- redistribute the stresses on perforations by changing their shape
  - elliptically shaped perforations

Elastic stress analysis

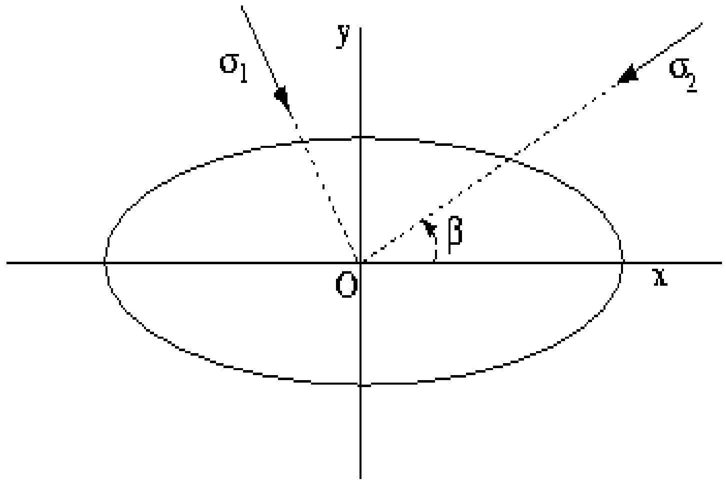

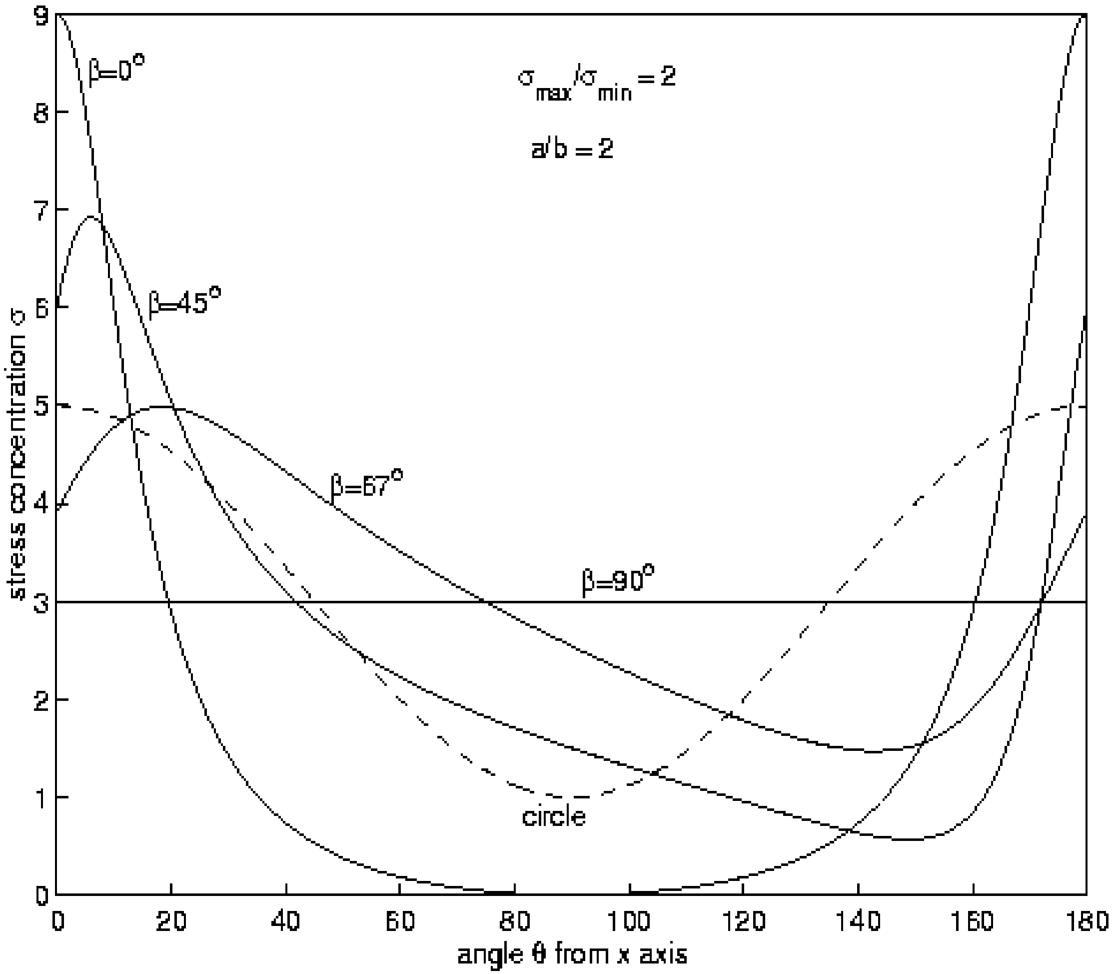

– uniform stress distribution if axis ratio is equal to the insitu stress ratio

– risk of perforation misalignment 23 degrees

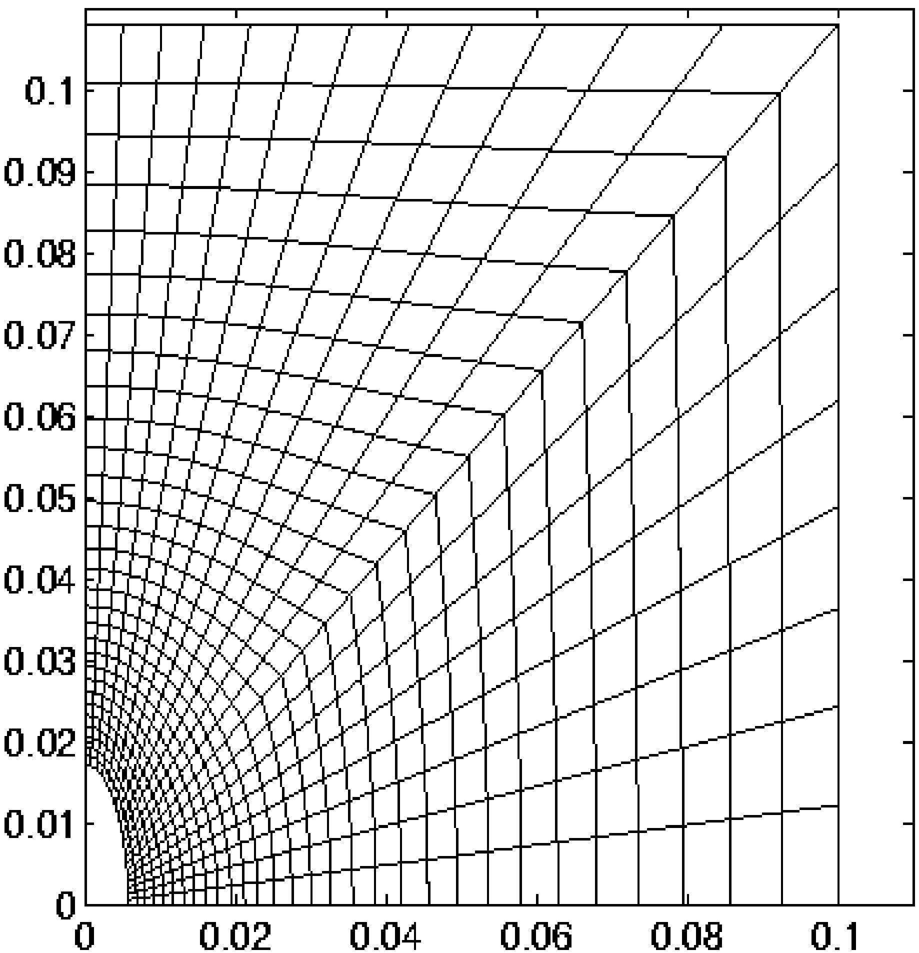

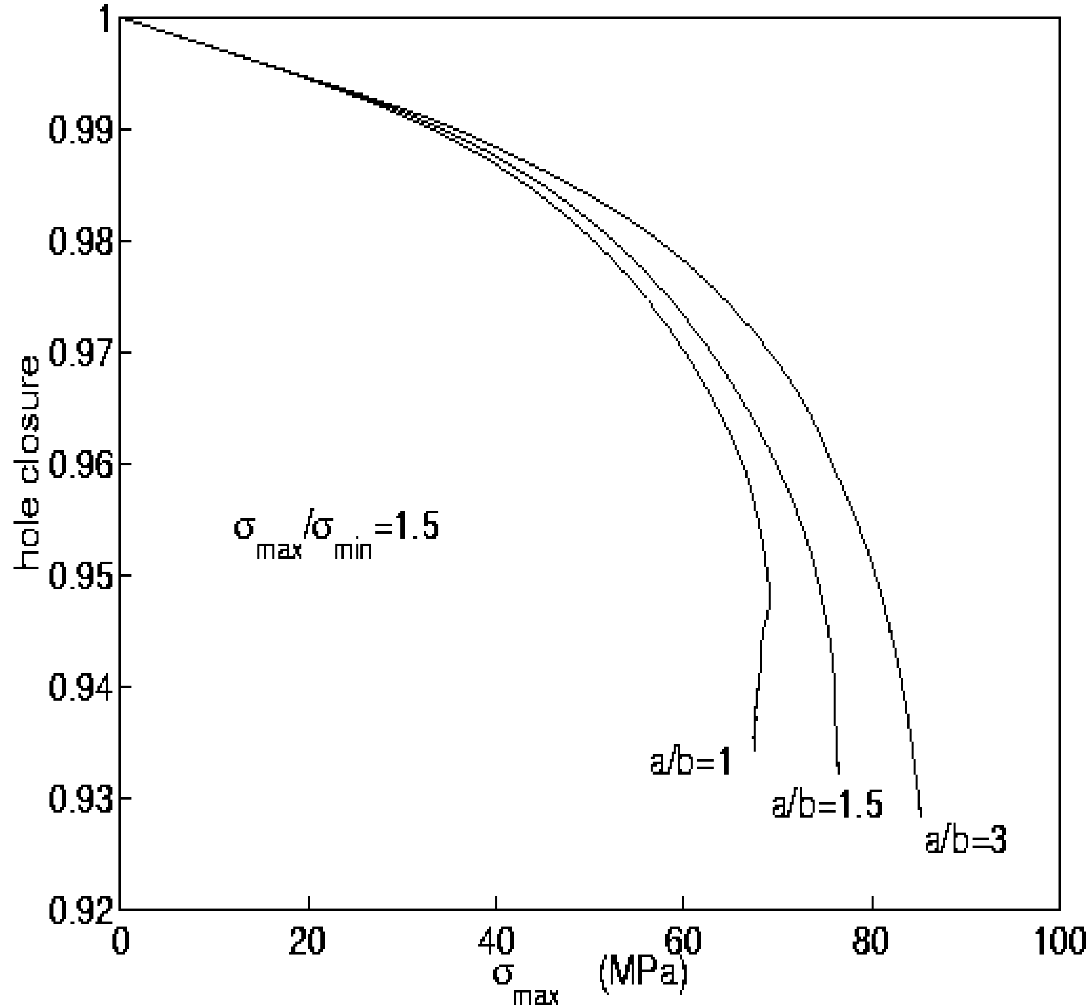

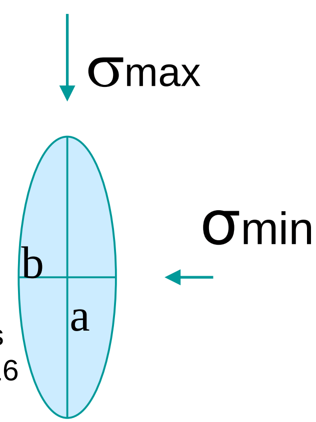

- compare cylindrical with elliptical perforations of the same cross-sectiona area (flow area)
- strongest perforations: ellipse with the highest axis ratio

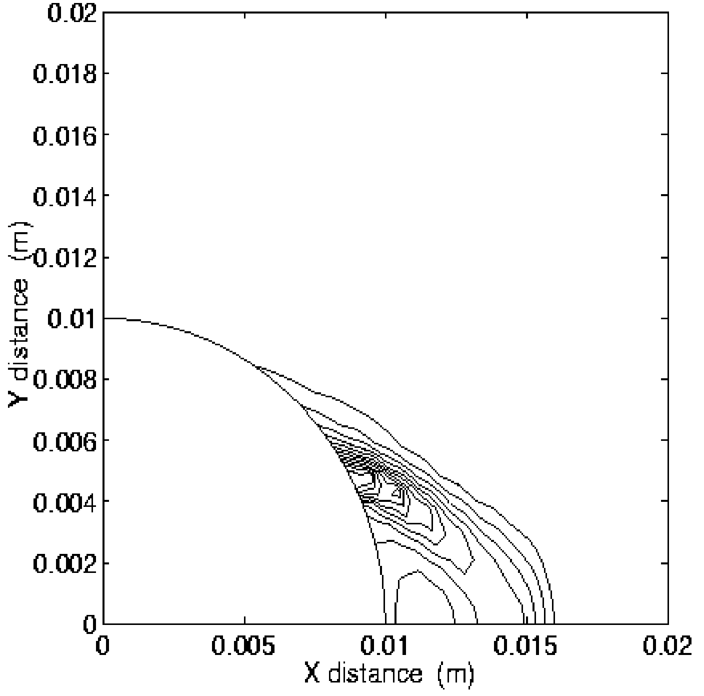

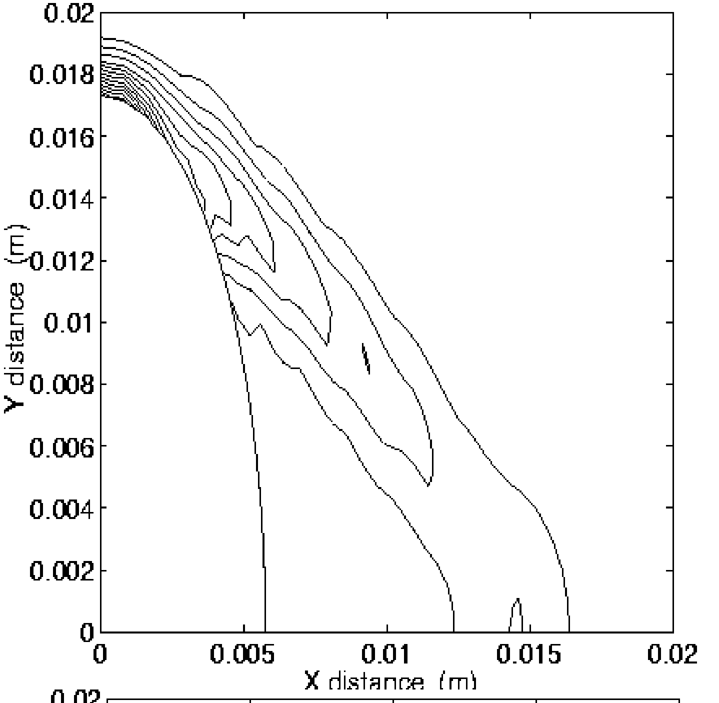

Plastic Strain

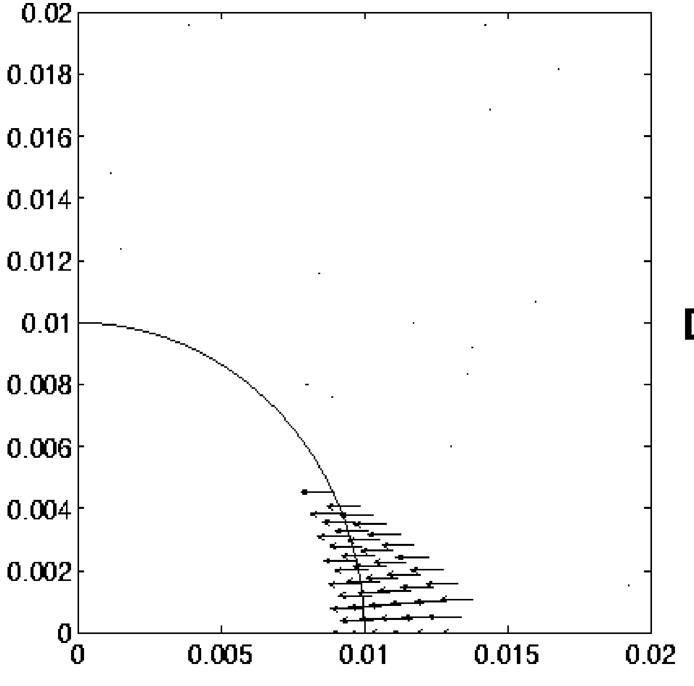

Displacement Field

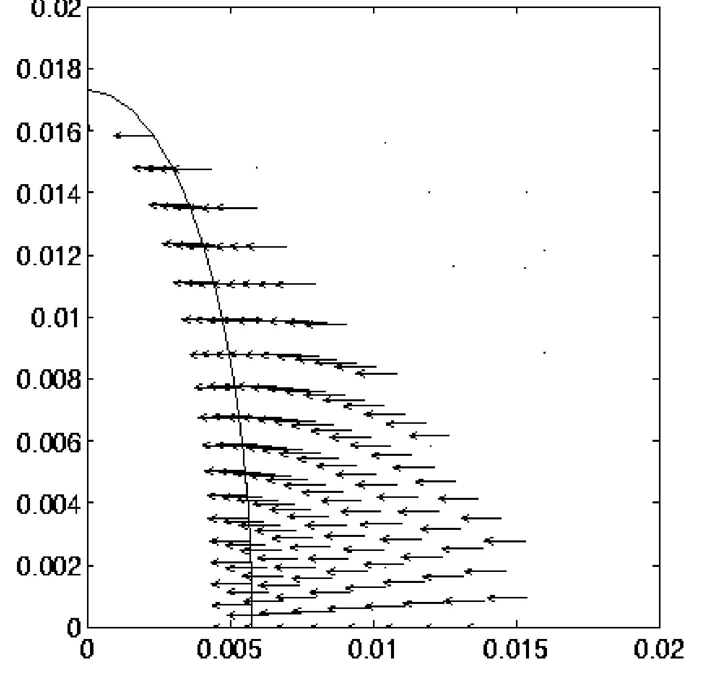

Conclusion

- elliptically shaped perforations are stronger than conventional perforations
- this result was found using Cosserat modelling
- results predicted by classical stress analysis were not applicable
- Cosserat allows for robust localization analysis
- Limited applications in design and practise

Introduction

A Gradient Plasticity
Motivation
Equations to satisfy
Consistency condition
Solution
Example

Gradient Elastoplasticity

Outlook

A Gradient Plasticity

Introduction
A Gradient Plasticity
Motivation
Equations to satisfy
Consistency condition
Solution
Example
Gradient Elastoplasticity
Outlook

Motivation

There are many gradient plasticity theories in the literature:

- Vardoulakis, Aifantis, de Borst and Pamin, Fleck and Hutchinson, Chambon, Zbib. . . (The list is non-exhaustive.)

It is impossible to review them all here.

- We will focus on numerical computations.

Biaxial test revisited

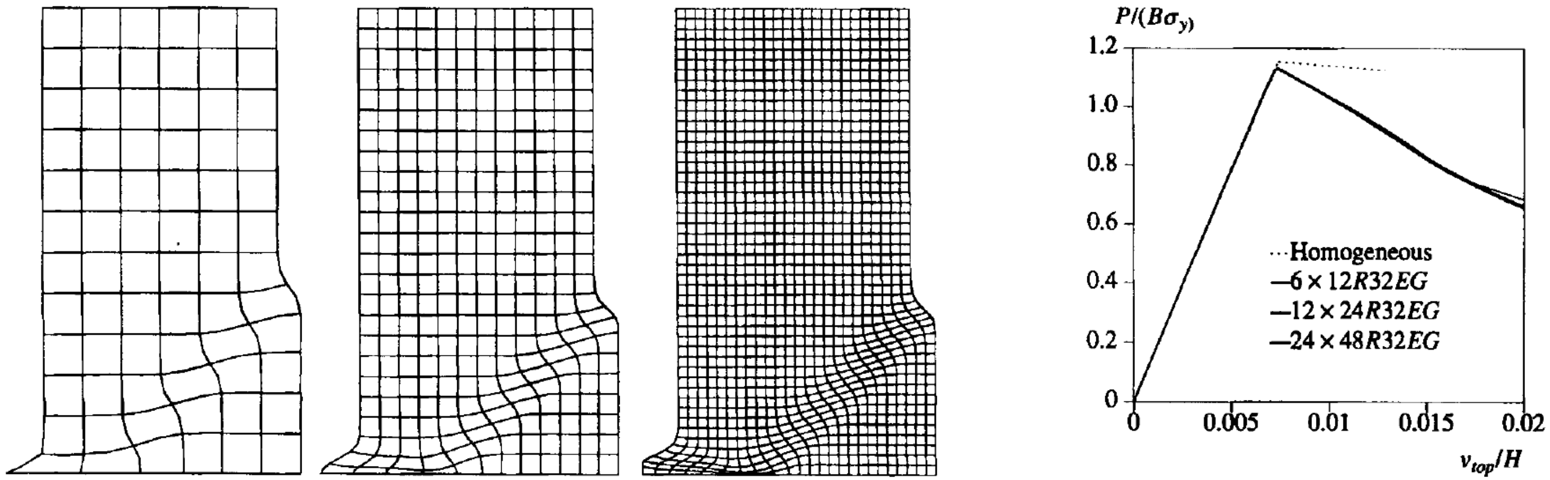

(de Borst and Pamin, 1996)

But:

- Equations change order at the elastoplastic boundary (this is inconvenient).
- The way of introducing the internal length is perhaps counter-intuitive.

Introduction
A Gradient Plasticity
Gradient Elastoplasticity
Motivation
Constitutive relations
Internal stress-like quantities
Finite element formulation
Biaxial test
Thick-cylinder test
Cavity expansion
Outlook

Gradient Elastoplasticity

Introduction
A Gradient Plasticity
Gradient Elastoplasticity
Motivation
Constitutive relations
Internal stress-like quantities
Finite element formulation
Biaxial test
Thick-cylinder test
Cavity expansion
Outlook

Motivation

Model deformation and failure of geomaterials.

- Significant irreversible (plastic) deformation.
- Strain softening leads to deformation localisation.
- Existence of scale effects.

Introduce microstructure in plasticity.

- Build on the ideas of gradient elasticity.
  - Governing equations do not change order.
  - No boundary conditions on elastoplastic boundary.

Gradient elastoplasticity

Total (equilibrium) stress rate

$$\dot{\sigma}_{ij} = C^e_{ijkl} \left(\dot{\epsilon}^e_{kl} - l_e^2 \nabla^2 \dot{\epsilon}^e_{kl} \right)$$

Yield function and plastic potential

$$F(\tau_{ij}, \psi) = 0, \quad Q(\tau_{ij}, \psi) = 0$$

Plastic strain rate

$$\dot{\epsilon}^p_{ij} = \dot{\psi} \frac{\partial Q}{\partial \tau_{ij}}$$

Reduced stress rate

$$\dot{\tau}_{ij} = \dot{\sigma}_{ij} - \dot{\alpha}_{ij}$$

Back stress rate

$$\dot{\alpha}_{ij} = -l_p^2 C^e_{ijkl} \nabla^2 \dot{\epsilon}^p_{kl}$$

C[1] finite elements:
triangles with 3 nodes and 36 dof

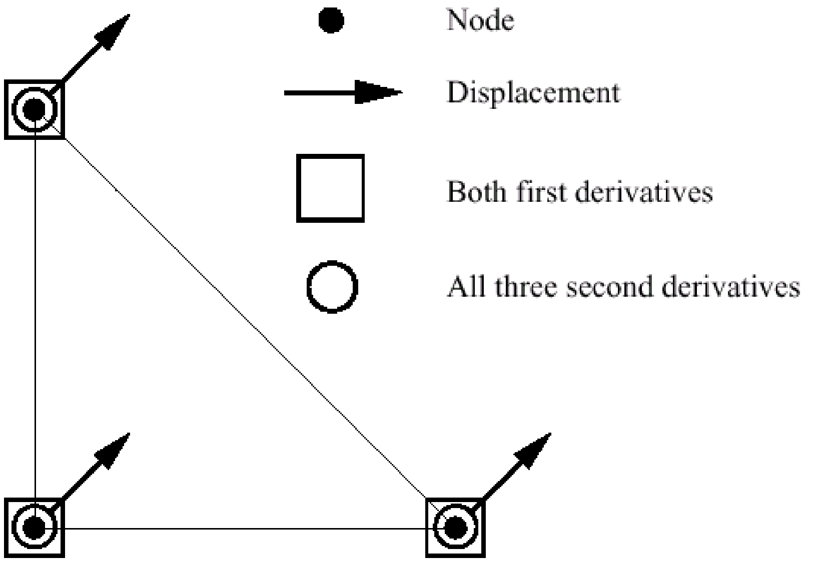

Introduction
A Gradient Plasticity
Gradient Elastoplasticity
Motivation
Constitutive relations
Internal stress-like quantities
Finite element formulation
Biaxial test
Thick-cylinder test
Cavity expansion
Outlook

Finite element formulation

- Use a displacement formulation: $u = N \cdot \hat{u}$
- Strain gradient in the weak form: C^1-continuous element.

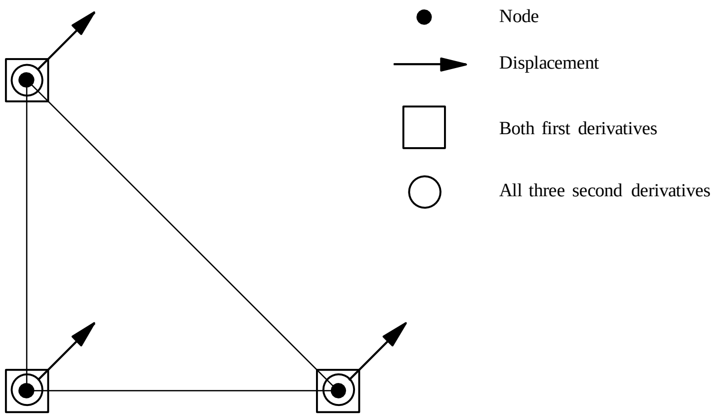

C^1 triangle.

- 36 degrees of freedom.
- Quintic polynomial.
- Cubic normal derivative.

Introduction
A Gradient Plasticity
Gradient Elastoplasticity
Motivation
Constitutive relations
Internal stress-like quantities
Finite element formulation
Biaxial test
Thick-cylinder test
Cavity expansion
Outlook

Modelling the biaxial test

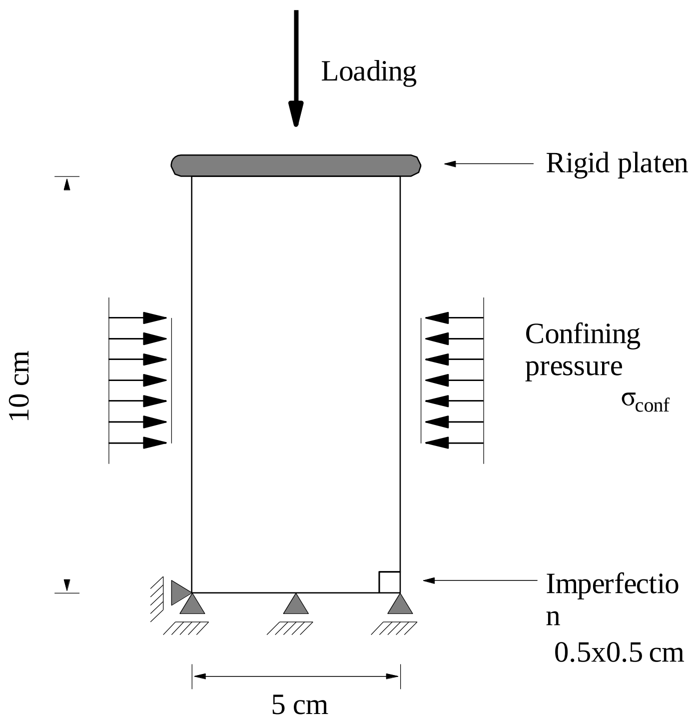

The different meshes used:

Name	Mesh	DOFs
Coarse	10x20	2772
Medium	20x40	10332
Fine	30x60	22692
Very fine	40x80	39852

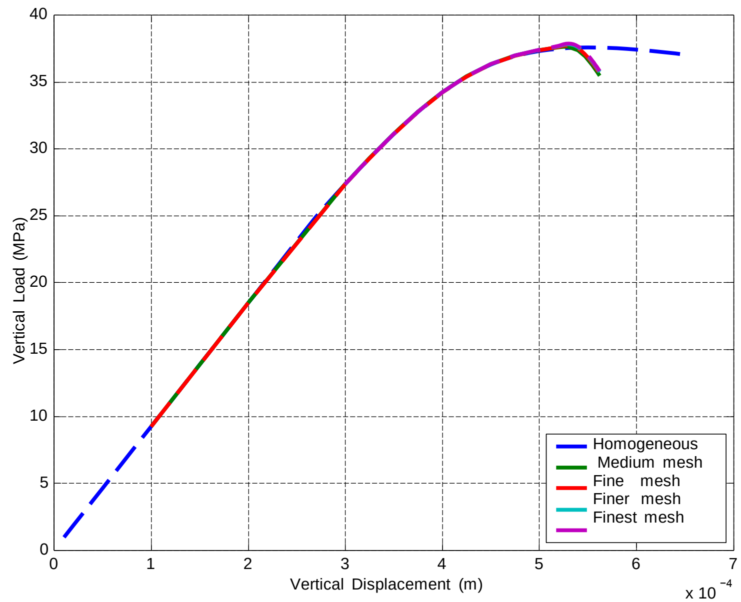

Introduction

A Gradient Plasticity

Gradient Elastoplasticity

Motivation
Constitutive relations
Internal stress-like quantities
Finite element formulation
Biaxial test
Thick-cylinder test
Cavity expansion

Outlook

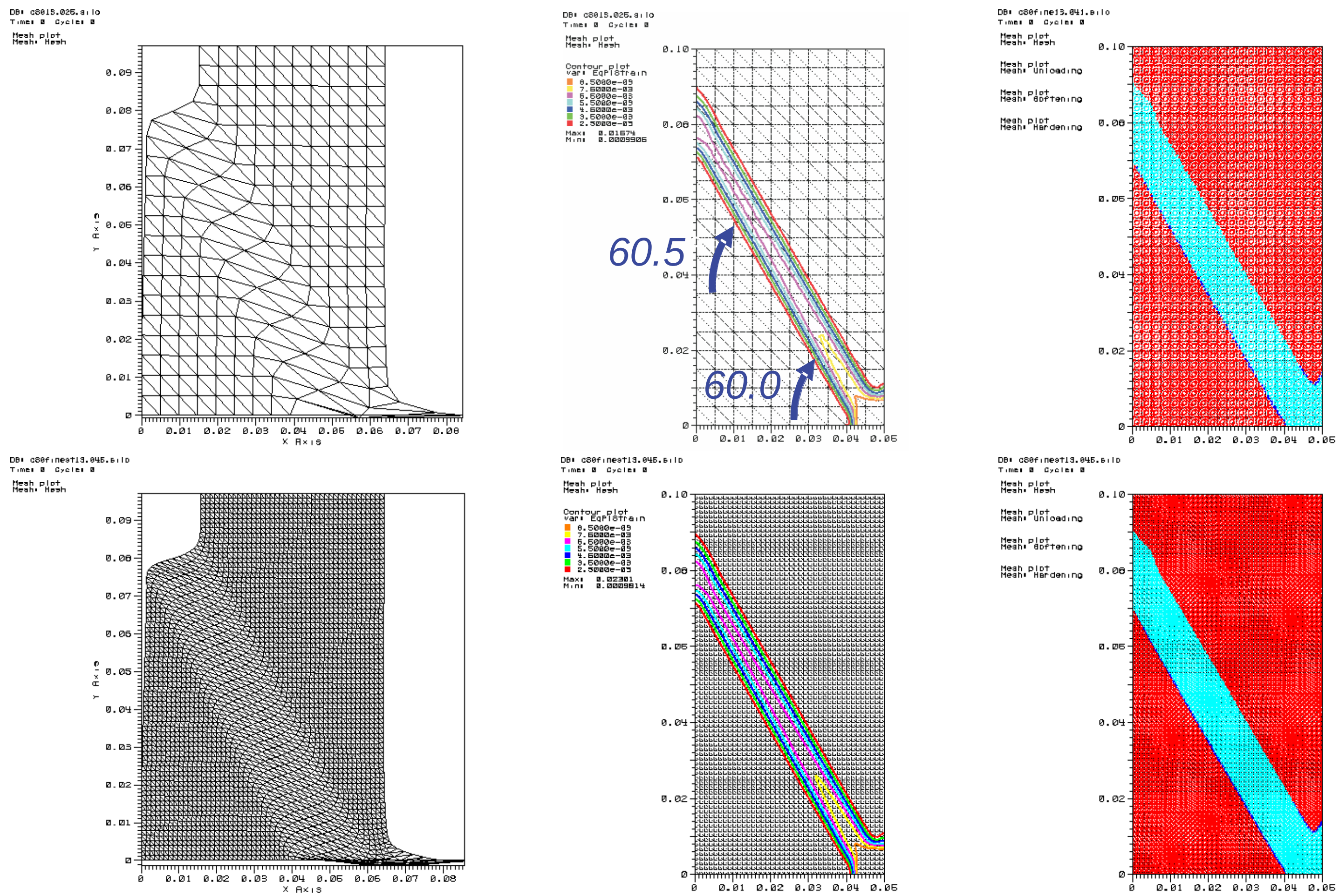

Displ. increment, plastic strain and material state. $\varphi = \psi = 32^0$

Introduction
A Gradient Plasticity
Gradient Elastoplasticity
Motivation
Constitutive relations
Internal stress-like quantities
Finite element formulation
Biaxial test
Thick-cylinder test
Cavity expansion
Outlook

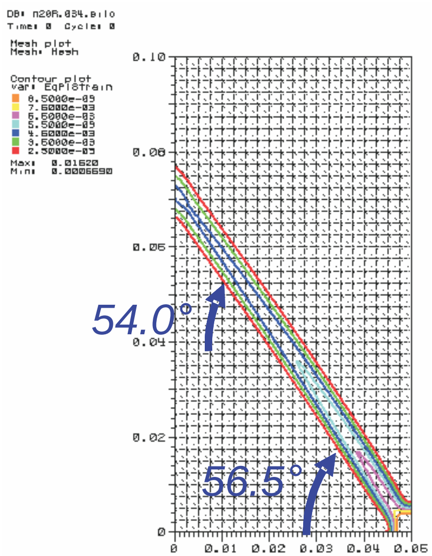

$\psi = 20^0$

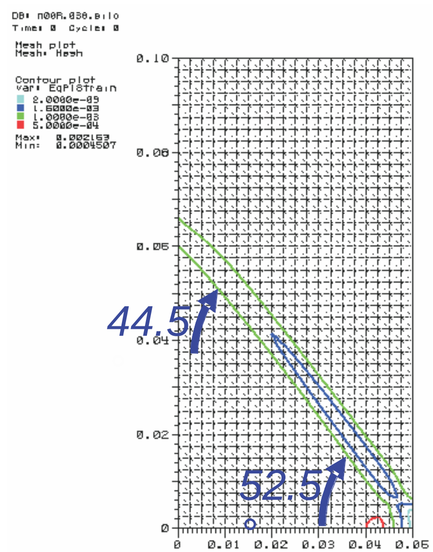

$\psi = 0^0$

Photo courtesy of I. Vardoulakis

Contours of plastic strain for different dilatancy angles.

- Simulations capture quantitatively the failure mechanism:
  - Shearband inclination: $\theta \approx 45^0 + (\varphi + \psi)/4$
  - Reorientation near a free boundary: $\theta \approx 45^0 + \psi/2$

Introduction
A Gradient Plasticity
Gradient Elastoplasticity
Motivation
Constitutive relations
Internal stress-like quantities
Finite element formulation
Biaxial test
Thick-cylinder test
Cavity expansion
Outlook

Modelling the thick-cylinder test

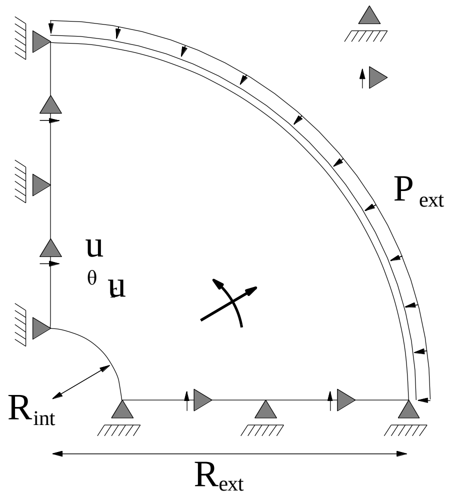

The different meshes used:

Name	Mesh	DOFs
Coarse	15x40	7380
Medium	20x80	19440
Fine	25x121	36300

- Stability of wellbores and perforations.
- External pressure increased to failure.

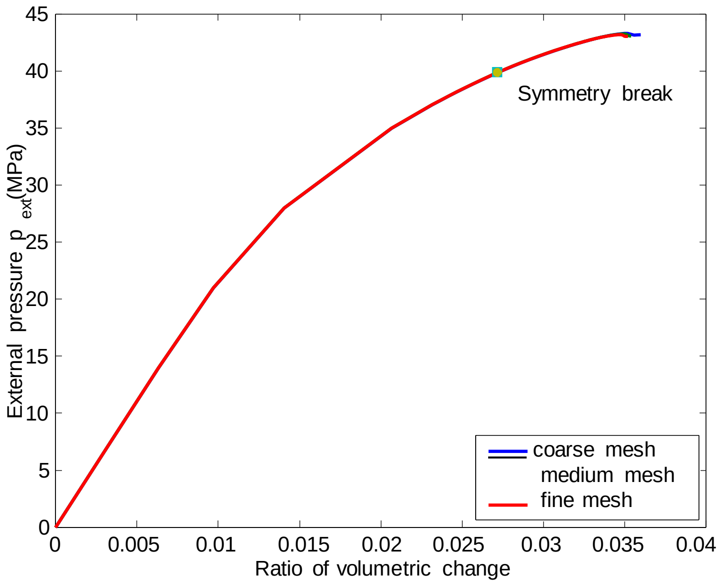

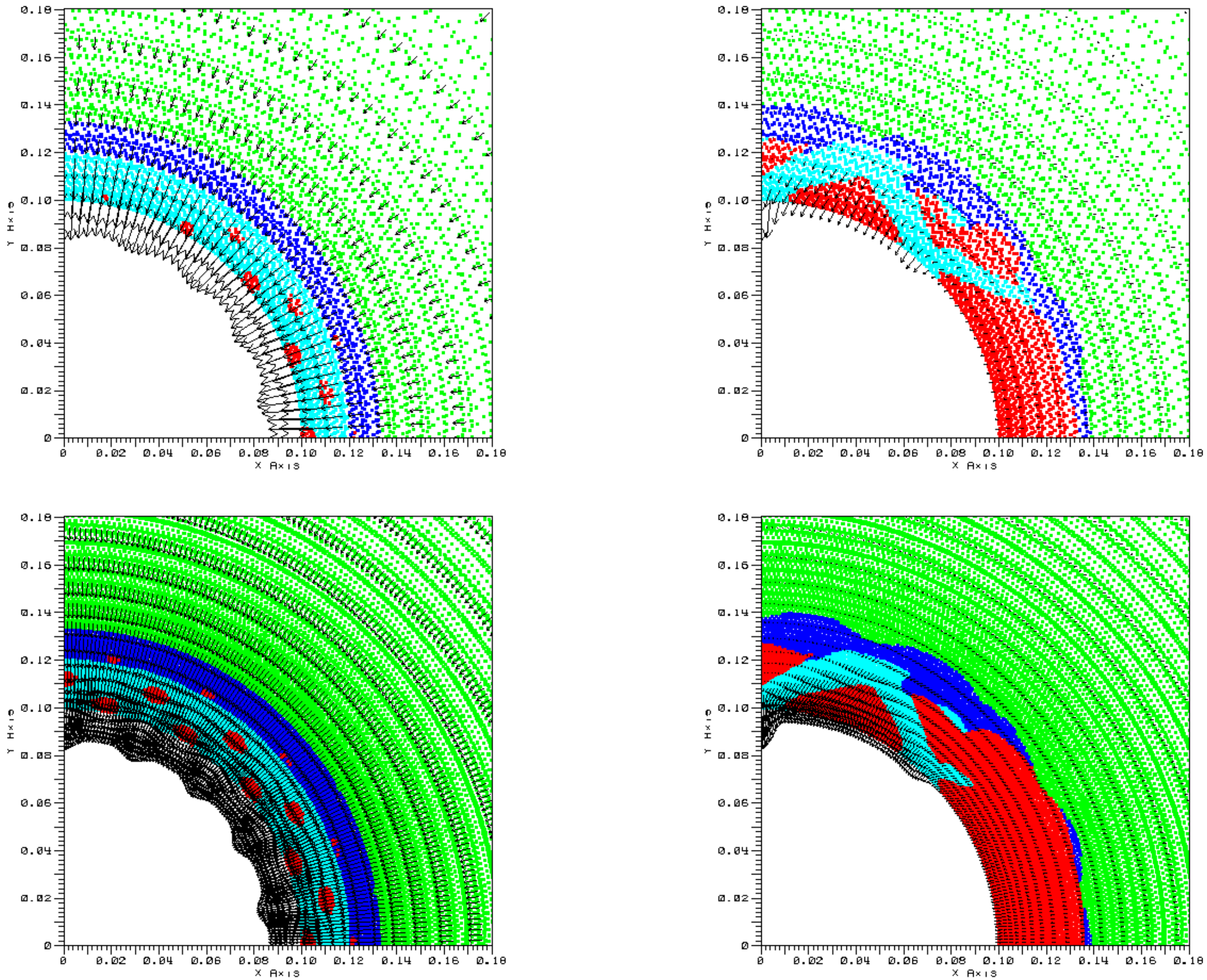

Loss of symmetry and final breakout mechanism.

Introduction

A Gradient Plasticity

Gradient Elastoplasticity

Motivation
Constitutive relations
Internal stress-like quantities
Finite element formulation
Biaxial test
Thick-cylinder test
Cavity expansion

Outlook

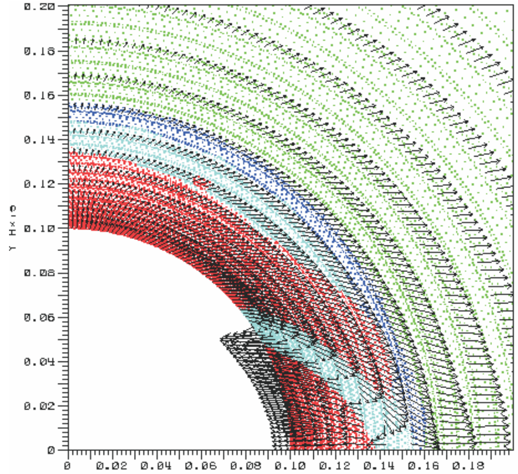

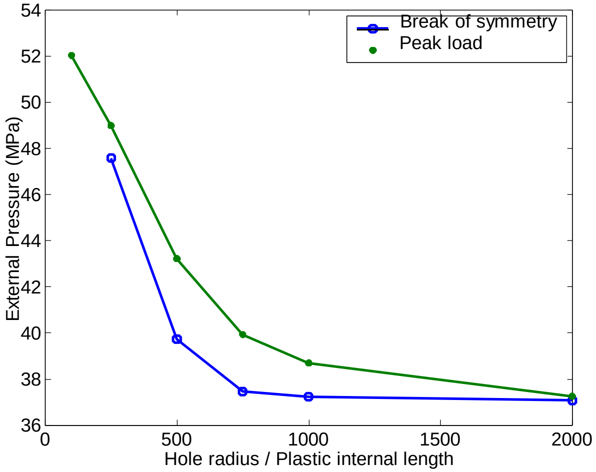

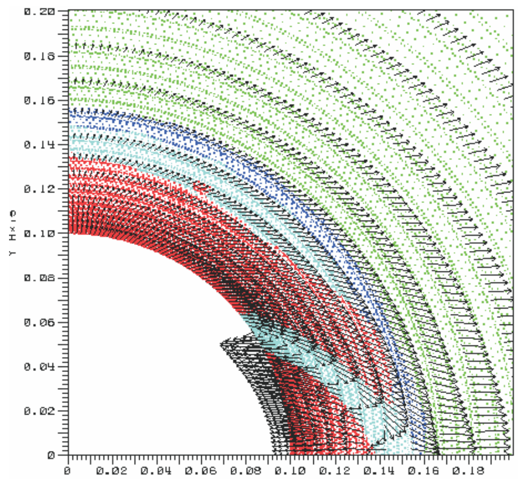

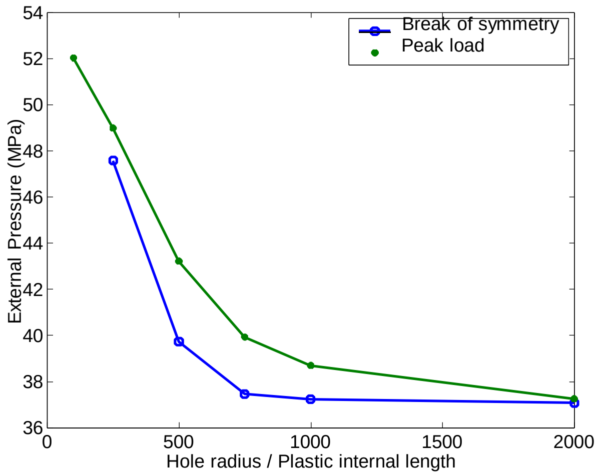

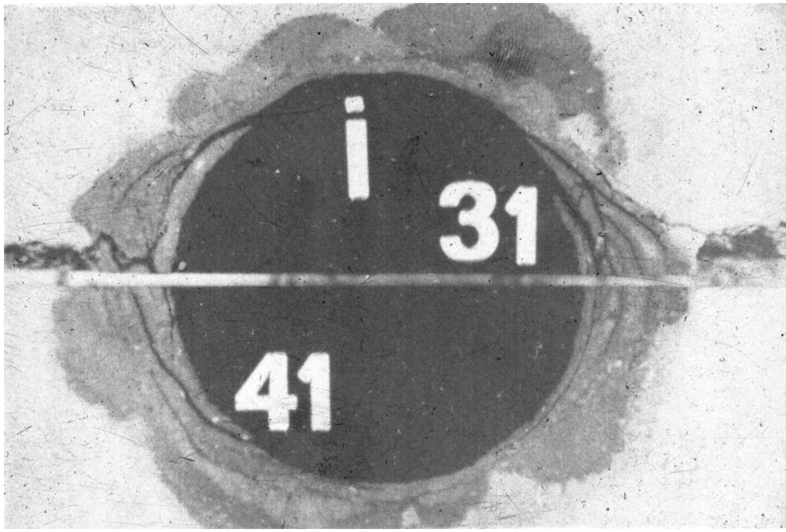

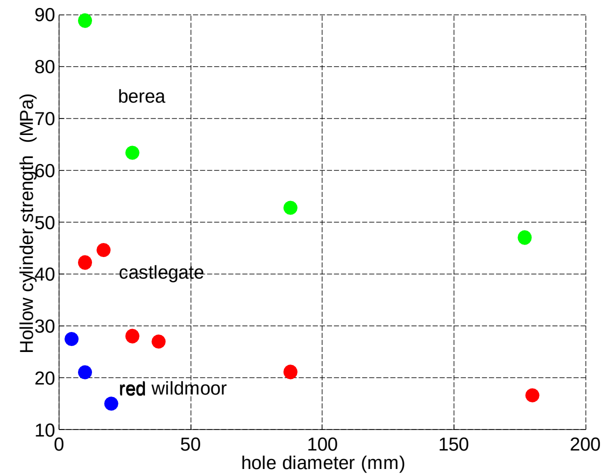

Photo courtesy of A. Guenot; scale effect data courtesy of E. Papamichos.

Introduction
A Gradient Plasticity
Gradient Elastoplasticity
Motivation
Constitutive relations
Internal stress-like quantities
Finite element formulation
Biaxial test
Thick-cylinder test
Cavity expansion
Outlook

Post-Bifurcation Analysis

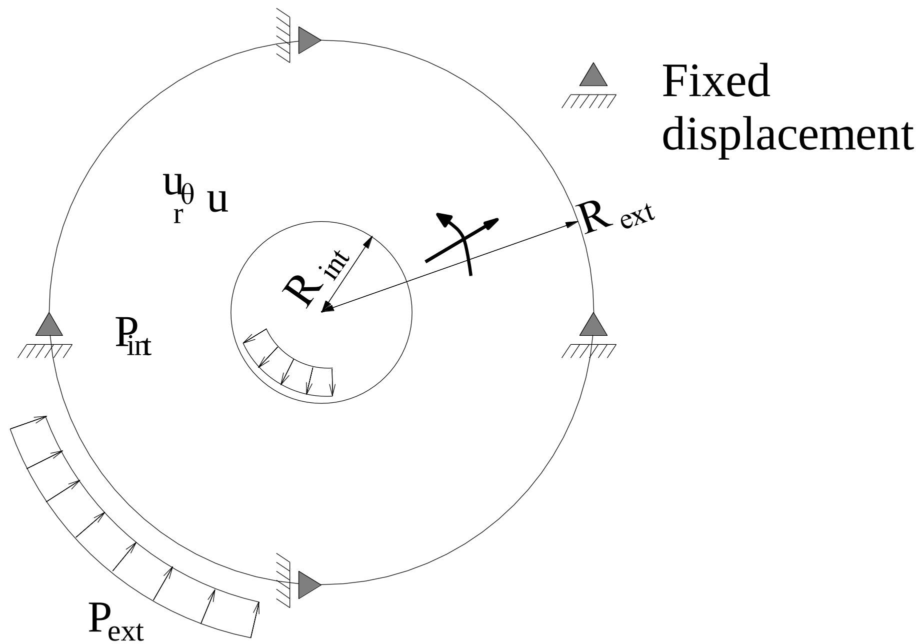

Finite element formulation

- Displacements: $\mathbf{u} = \mathbf{N} \cdot \hat{\mathbf{u}}$
- $\mathbf{u}$ must be C^1 continuous
- We use a C^1 triangle (36 DOFs)

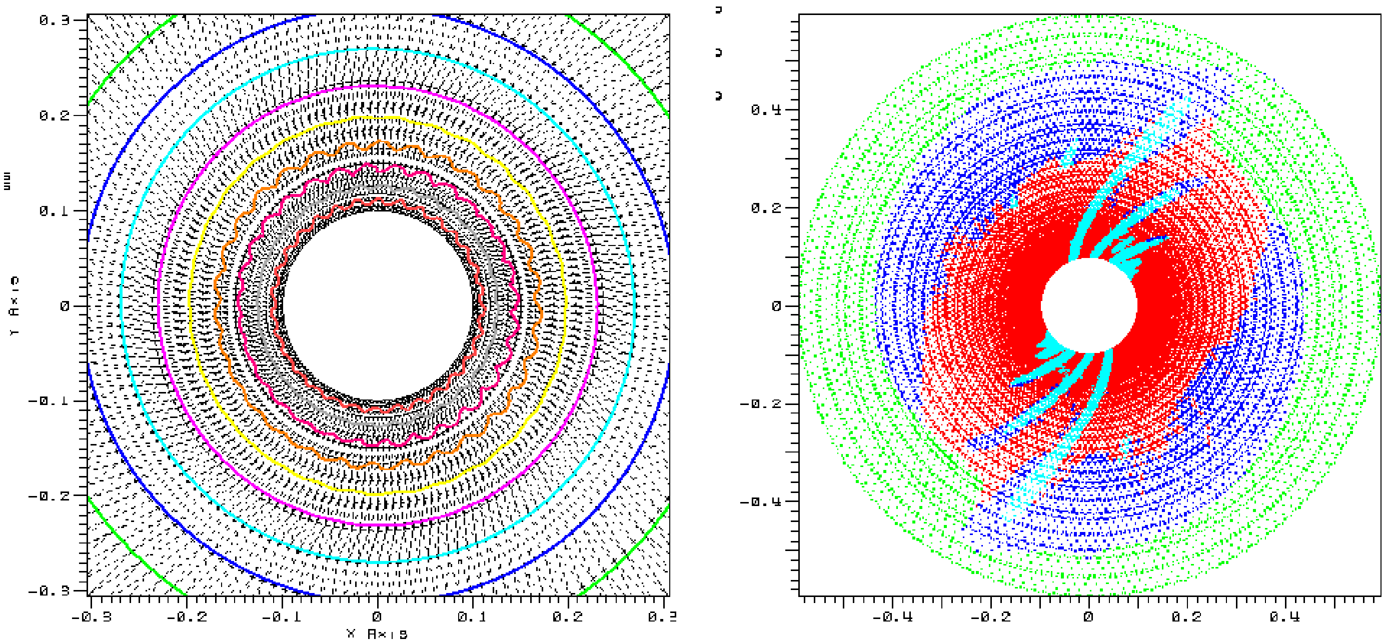

(a) Displ. increment (b) Final material state

For the case of $R_i = 10$ cm and a mesh with 32640 DOFs

- Spontaneous loss of axisymmetry, $m = 30$
- Deformation localisation in thin, softening bands

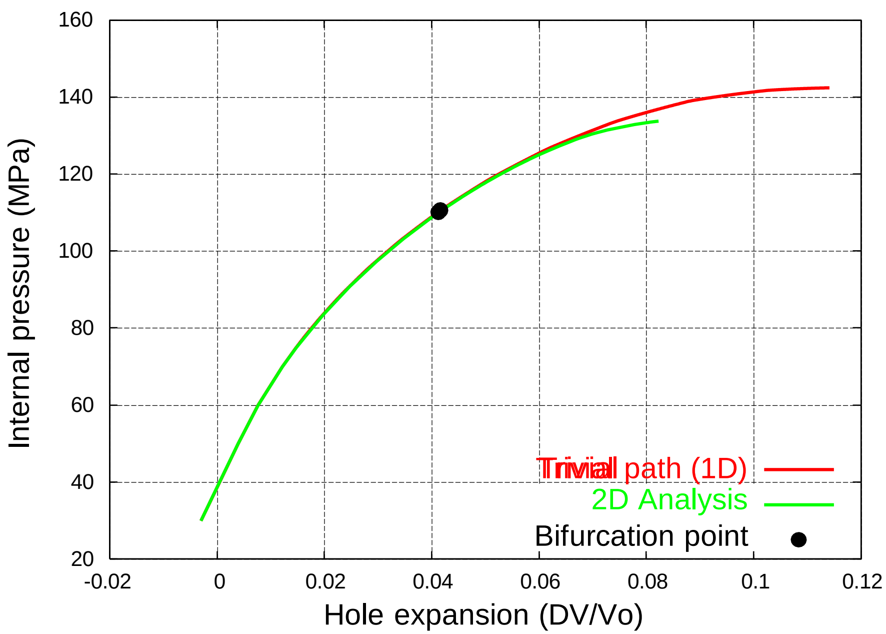

(a) Deformation paths

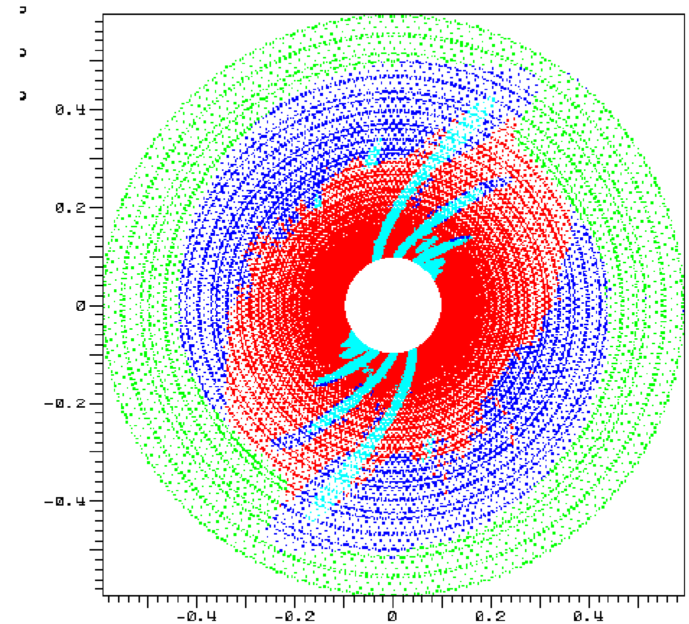

(b) Final material state

For the case of $R_i = 10$ cm and a mesh with 32640 DOFs

- Spontaneous loss of axisymmetry, m = 30
- Deformation localisation in thin, softening bands
- The maximum pressure is lower than the limit pressure

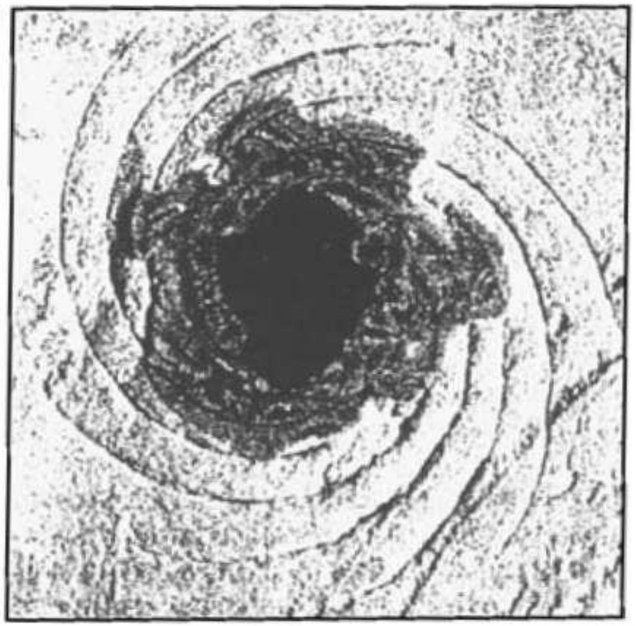

(a) (van den Hoek, 2001)

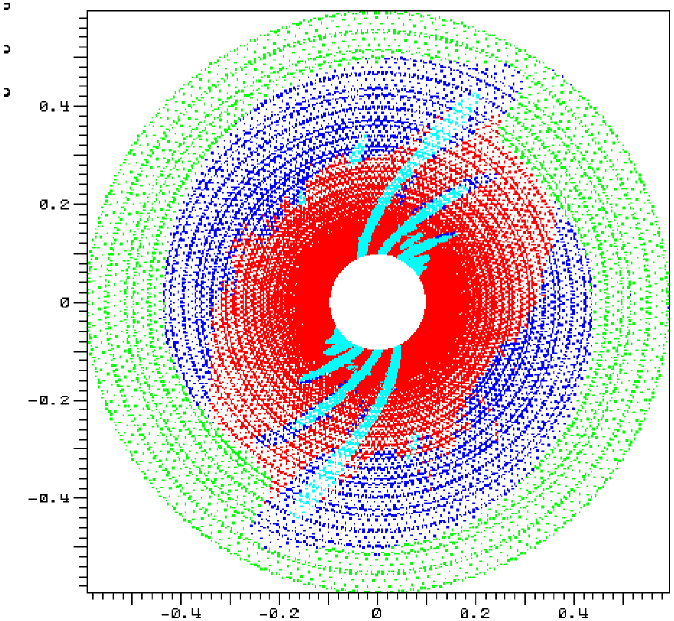

(b) Final material state

For the case of R_i = 10 cm and a mesh with 32640 DOFs

- Spontaneous loss of axisymmetry, m = 30
- Deformation localisation in thin, softening bands
- The maximum pressure is lower than the limit pressure

Introduction

A Gradient Plasticity

Gradient Elastoplasticity

Outlook

Outlook

Introduction
A Gradient Plasticity
Gradient Elastoplasticity
Outlook

Outlook

Higher order theories:

- Introduce material length scales.
- Regularise material behaviour in the softening regime.
- Are able to capture localised failure mechanisms.
  - Finite shearband thickness.
  - Robust numerical solutions post-peak.
  - Robust predictions and tracking of instabilities.
- Are able to capture scale effects.

However there are still issues to be resolved. . .

Introduction
A Gradient Plasticity
Gradient Elastoplasticity
Outlook

. . . and some of these issues are:

- New parameters: material lengths and softening rate.
  - How do we calibrate?
  - Element tests are NOT the answer!

. . . and some of these issues are:

- New parameters: material lengths and softening rate.
  - How do we calibrate?
  - Element tests are NOT the answer!
- New types of boundary conditions: richer behaviour.
  - Physical meaning not always clear.
  - Restriction of derivatives is analogous to “roughness”.